

Review

Tripartite Entanglement: Foundations and Applications

Márcio M. Cunha ¹, Alejandro Fonseca ² and Edilberto O. Silva ^{1,*}

¹ Departamento de Física, Universidade Federal do Maranhão, São Luís 65085-580, Maranhão, Brazil; marciomc05@gmail.com

² Departamento de Física, Universidade Federal de Pernambuco, Recife 50670-901, Pernambuco, Brazil; alejofonseca4@gmail.com

* Correspondence: edilberto@gmail.com or edilberto.silva@ufma.br

Received: 29 August 2019; Accepted: 1 October 2019; Published: 9 October 2019



Abstract: We review some current ideas of tripartite entanglement. In particular, we consider the case representing the next level of complexity beyond the simplest (though far from trivial) one, namely the bipartite case. This kind of entanglement plays an essential role in understanding the foundations of quantum mechanics. It also allows for implementing several applications in the fields of quantum information processing and quantum computing. In this paper, we review the fundamental aspects of tripartite entanglement focusing on Greenberger–Horne–Zeilinger and W states for discrete variables. We discuss the possibility of using it as a resource to execute quantum protocols and present some examples in detail.

Keywords: quantum mechanics; quantum entanglement; tripartite entanglement; GHZ states; W states

1. Introduction

Quantum entanglement is one of the most astonishing aspects of quantum mechanics, initially, by virtue of its deep implications in the context of the theory itself and more recently due to the large amount of applications within the emerging fields of quantum information processing [1] and quantum computation¹.

The most well-known type of entanglement involves two parts sharing a pair of qubits, the so-called EPR (after Einstein Podolsky Rosen) or Bell states² [3]. Nevertheless, note that two parts may also share an entangled state in larger dimensions, such as qutrits [4] and/or subsystems in continuous variables. Besides the relevance of bipartite entanglement in the understanding of quantum foundations and quantum information science, the search of entangled states involving more than two qubits is also desirable. After all, it may provide useful insights regarding fundamental aspects of the theory itself, offering in this way new possibilities in the development of applications such as protocols in quantum information [5]. Moreover, the usage of genuine multipartite entanglement often displays several advantages in comparison to bipartite entanglement [6]. For instance, it is possible to establish quantum networks with multi-users, execute quantum computation with cluster states [7,8] and perform measurement-based quantum computing [9]. These kinds of entangled states can be used, for instance, as a quantum channel to establish quantum communication between several separated

¹ Note that entanglement is not the only nonclassical resource useful for computation, though.

² It is important to keep in mind that *bipartite entanglement* does not necessarily imply two spatially separated parts. Instead, it can be generated between different degrees of freedom in a single part [2].

locations. An introduction to multipartite entanglement can be found in [10]. In [11], a study of maximally multipartite entangled states was carried out. In [12], entanglement in many-body systems is reviewed, including aspects of multipartite entanglement in that scenario. A general review about multipartite entanglement can be found in [13].

The simplest case of multipartite entanglement is tripartite entanglement that involves three-parts. This kind of entanglement play an essential role in the development of aspects such as quantum nonlocality and has a large number of applications in quantum information protocols. In this review, we explore the main features of tripartite entanglement focusing our attention on Greenberger-Horne-Zeilinger (hereafter GHZ) and the so called W states. We discuss the most fundamental aspects and applications.

The paper is organized in the following way: In Section 2, we give a brief overview of bipartite entanglement. In Section 3, we discuss tripartite entanglement and define the corresponding classes of entanglement for qubits. Then, we review some aspects of quantum nonlocality and tripartite entanglement in Section 4. In Section 5, we provide several examples of quantum information protocols employing tripartite entanglement. We review the main aspects of these applications, illustrating the corresponding schemes. In Section 6, we list several proposals for how to experimentally produce tripartite entanglement in the literature. Then, we devote time to briefly exploring some aspects related to detection and characterization of tripartite entanglement in Section 7. In Section 8, we consider the topic of remote preparation of quantum states. In Section 9, we examine some aspects of tripartite entanglement involving continuous variables. The effects of noisy environments are considered in Section 10. Finally, we emphasize the main conclusions in Section 11.

2. Overview of Bipartite Entanglement

For the sake of completeness, let us quickly review some important aspects of entanglement between two parts. We start by describing the case of pure states and then we cite some of the most important entangled mixed states.

2.1. Pure States

Due to the Schmidt decomposition, any quantum state shared between two parts, say Alice and Bob as usual, may be written as $|\psi\rangle = \sum_{j=0}^{d-1} \sqrt{\lambda_j} |\phi_A\rangle_j \otimes |\phi_B\rangle_j = \sum_{j=0}^{d-1} \sqrt{\lambda_j} |j, j\rangle$, with Schmidt coefficients $\lambda_j \in \mathbb{R}$, satisfying $\sum_{j=0}^{d-1} \lambda_j = 1$ and $d = \min(\dim \mathcal{H}_A, \dim \mathcal{H}_B)$, where \mathcal{H}_k is the Hilbert space associated with the k -th part. In particular, it is possible to say that $|\psi\rangle$ is entangled whenever there exists more than one nonzero Schmidt coefficient. Furthermore, we can define a basis for the Hilbert space associated with both parts $\mathcal{H}_{AB} = \mathcal{H}_A \otimes \mathcal{H}_B$, composed by d^2 elements given by:

$$|\phi_{mn}^{(d)}\rangle = \sum_{k=0}^{d-1} \beta_{km} |k, k \oplus n\rangle, \quad m, n = 0, \dots, d-1, \tag{1}$$

where the symbol “ \oplus ” denotes a sum modulo d , the β_{km} coefficients control how entangled the basis is and satisfy the relation $\sum_{k=0}^{d-1} \beta_{km} \beta_{km'}^* = \delta_{mm'}$. In particular, for $d = 2$, the basis can be parametrized as [14]:

$$\begin{aligned} |\phi_{00}^{(2)}\rangle &= \cos \theta |00\rangle + \sin \theta |11\rangle, & |\phi_{10}^{(2)}\rangle &= \sin \theta |00\rangle - \cos \theta |11\rangle, \\ |\phi_{01}^{(2)}\rangle &= \cos \theta |01\rangle + \sin \theta |10\rangle, & |\phi_{11}^{(2)}\rangle &= \sin \theta |01\rangle - \cos \theta |10\rangle, \end{aligned}$$

with $0 \leq \theta \leq \pi/2$. Moreover, any element of the basis with $\beta_{km} = \omega_d^{k \cdot m} / \sqrt{d}$, corresponds to a maximally entangled state, where $\omega_d = \exp(2\pi i/d)$ is the primitive d -th root of unity. Explicitly, it is known as the Bell or EPR³ basis for $d = 2$ and is written as:

$$|\phi^\pm\rangle = \frac{1}{\sqrt{2}} (|00\rangle \pm |11\rangle), \quad |\psi^\pm\rangle = \frac{1}{\sqrt{2}} [|01\rangle \pm |10\rangle]. \tag{2}$$

Hereafter, $|\phi_{mn}^{(d)}\rangle$ denotes a maximally entangled state, for the sake of simplicity.

An important feature is that any Bell state can be converted into another one by using local unitary transformations and classical communication (hereafter LOCC) only. Moreover, it has been shown that these states can be used to develop several informational tasks such as superdense coding [16] and quantum teleportation [17] with the highest attainable performance [18,19]. They also represent a very useful resource for testing fundamental aspects of the quantum world.

2.2. Some Special Families of Mixed States

Suppose Alice and Bob have a source of entangled qubits prepared in a state $\hat{\rho}$. Then, Alice applies a unitary operation \hat{U} chosen at random and informs Bob to carry out either \hat{U} or \hat{U}^* on his qubit. Regardless of the initial state of the system, after many repetitions of the same procedure, the final state shared by Alice and Bob reduces to a Werner or an isotropic state.

2.2.1. Werner States

When Alice and Bob apply local operations $\hat{U} \otimes \hat{U}$, we have [20]:

$$\hat{\rho} \rightarrow \int \hat{U} \otimes \hat{U} \hat{\rho} \hat{U}^\dagger \otimes \hat{U}^\dagger dU = \hat{\rho}_W, \tag{3}$$

where dU is the Haar measure of the unitary group $U(d)$ and $\hat{\rho}_W$ is the Werner state, given by:

$$\hat{\rho}_W = (1 - p) \frac{2}{d^2 + d} \hat{P}^{(+)} + p \frac{2}{d^2 - d} \hat{P}^{(-)}, \tag{4}$$

with $\hat{P}^{(\pm)} = \frac{1}{2} (\hat{1} \pm \hat{V})$, where $\hat{1}$ is the identity: $\hat{1} = \sum_{jk=0}^{d-1} |jk\rangle\langle jk|$ and \hat{V} is the flip operator: $\hat{V} = \sum_{jk=0}^{d-1} |jk\rangle\langle kj|$. It is important to mention that the Werner state $\hat{\rho}_W$ is invariant under $\hat{U} \otimes \hat{U}$ operations. By using the following relations $\hat{P}^{(+)}\hat{P}^{(-)} = 0$, $\hat{P}^{(\pm)2} = \hat{P}^{(\pm)}$ and $\text{tr} \hat{P}^{(-)} = \frac{1}{2}(\text{tr} \hat{1} - \text{tr} \hat{V}) = \frac{1}{2}(d^2 - d)$, it is easy to show that the operation-invariant p^5 is equal to $p = \text{tr}(\hat{P}^{(-)}\hat{\rho}_W)$.

2.2.2. Isotropic States

In the case of local operations $\hat{U} \otimes \hat{U}^*$, the state $\hat{\rho}$ is transformed as [21]:

$$\hat{\rho} \rightarrow \int \hat{U} \otimes \hat{U}^* \hat{\rho} (\hat{U} \otimes \hat{U}^*)^\dagger dU = \hat{\rho}_f, \tag{5}$$

where $\hat{\rho}_f$ is the isotropic state, given by:

$$\hat{\rho}_f = \frac{1 - f}{d^2 - 1} \hat{1} + \frac{fd^2 - 1}{d^2 - 1} \hat{P}_+, \tag{6}$$

³ EPR, after Einstein's, Podolsky's, and Rosen's seminal paper [15].

⁴ The symbol "*" indicates complex conjugation of the associated matrix elements.

⁵ In the case $d = 2$, in particular, p denotes the singlet fraction or, in other words, the degree of similarity of the state before ($\hat{\rho}$) and after (\hat{W}_p) applying twirling operations to the singlet state $|\phi_{11}^2\rangle$, i.e., $p = \text{tr}(|\phi_{11}^2\rangle\langle\phi_{11}^2| \hat{\rho}) = \text{tr}(|\phi_{11}^2\rangle\langle\phi_{11}^2| \hat{W}_p)$.

with $\hat{P}_+ = |\phi_{00}^{(d)}\rangle\langle\phi_{00}^{(d)}|$. Analogously to the Werner state, the isotropic state is invariant under $\hat{U} \otimes \hat{U}^*$ operations.

By expanding the identity operator in the generalized Bell basis $\hat{1} = \sum_{\mu\nu=0}^{d-1} |\phi_{\mu\nu}^{(d)}\rangle\langle\phi_{\mu\nu}^{(d)}|$, the isotropic state takes the following form:

$$\hat{\rho}_f = f |\phi_{00}^{(d)}\rangle\langle\phi_{00}^{(d)}| + \frac{1-f}{d^2-1} \sum_{\substack{\mu\nu=0 \\ (\mu,\nu)\neq(0,0)}}^{d-1} |\phi_{\mu\nu}^{(d)}\rangle\langle\phi_{\mu\nu}^{(d)}|. \tag{7}$$

In this expression, it is possible to see more clearly that the operation invariant f is equal to: $f = \text{tr}(|\phi_{00}^{(d)}\rangle\langle\phi_{00}^{(d)}| \hat{\rho}) = \text{tr}(|\phi_{00}^{(d)}\rangle\langle\phi_{00}^{(d)}| \hat{\rho}_f)$. Due to their properties, these states have been very useful to unveil the relation between the concepts of entanglement and Bell nonlocality [22,23]. Several proposed generalizations to the multipartite case are presented later in this review.

3. Tripartite Entanglement

3.1. Genuine Tripartite Pure States

When dealing with tripartite quantum systems, it is possible to write the associated state $|\Psi\rangle$ in one out of three ways: totally separable $|\Psi\rangle = |\psi_A\rangle \otimes |\psi_B\rangle \otimes |\psi_C\rangle$, in terms of biseparable partitions $|\Psi\rangle = |\psi_j\rangle \otimes |\psi_{kl}\rangle$ ($\{j, k, l\} = \{A, B, C\}$) or genuinely entangled, which will be explained in the next part. In [24], Zhao and collaborators provide a set of methods based on expectation values of Pauli operators to identify the class of a given state. The possible configurations are presented in Figure 1.

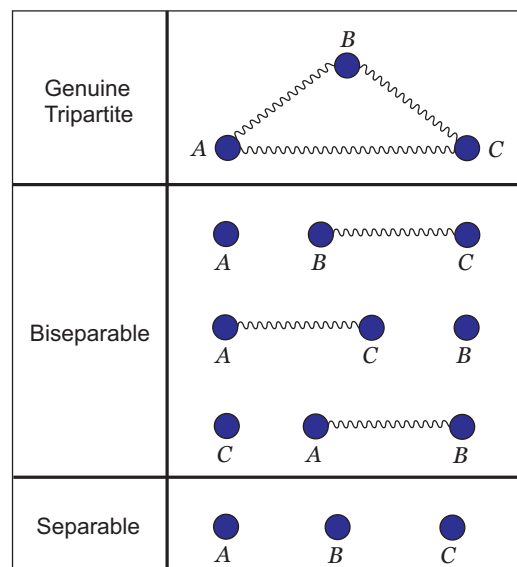


Figure 1. Possible scenarios of three-qubit quantum states. From top to bottom: First, Genuine tripartite entanglement, where all qubits are in an entangled state. Second, biseparable partitions, where only two qubits are entangled. Third, full separable state.

It is a well-known fact that it is possible to transform any state from the Bell basis into another one by using LOCC only, or to another arbitrary state of two qubits with nonzero probability [25,26]. However, a very interesting feature emerges when we deal with quantum systems involving more than two qubits: different classes of entanglement arise. For the simplest instance, namely three qubits, there are two nonequivalent classes of entanglement: GHZ states [27,28] and W states [29], defined as:

$$|GHZ\rangle = \frac{1}{\sqrt{2}} (|000\rangle + |111\rangle), \quad |W\rangle = \frac{1}{\sqrt{3}} (|001\rangle + |010\rangle + |100\rangle). \tag{8}$$

These two classes are totally nonequivalent under Stochastic Local Operations and Classical Communication (hereafter SLOCC). It means that it is impossible to convert any state of a given class into one of another class and vice versa. Thus, GHZ and W states constitute genuinely entangled states for the case of three qubits.

The idea of GHZ entanglement by itself has its deep origins in the foundations of quantum theory. In fact, this family of states was proposed to investigate quantum nonlocality beyond Bell's Theorem [28]. Furthermore, as shown in [30], the premises of the EPR argument about the incompleteness of quantum theory are also inconsistent when applied to GHZ states. As discussed in more detail in the next section, employing GHZ states enabled a demonstration of the incompatibility between the predictions of local realism and quantum mechanics without demanding the usage of an inequality [3].

As in the bipartite case, it is also possible to write a GHZ state with an arbitrary amount of entanglement⁶. In this case, we start by defining the state:

$$|\psi_{000}\rangle = \cos \theta |000\rangle + \sin \theta |111\rangle, \tag{9}$$

with $\theta = \{0, \pi/2\}$. From local operations on $|\psi_{000}\rangle$, we can construct a GHZ basis. These states are given by:

$$|\psi_{\mu\lambda\omega}\rangle = \sum_{j=0}^1 (-1)^{\mu j} b_{\mu \oplus j} |j, j \oplus \lambda, j \oplus \omega\rangle, \tag{10}$$

where $b_0 = \cos \theta$ e $b_1 = \sin \theta$. They can be written more explicitly as:

$$|\psi_{000}\rangle = \cos \theta |000\rangle + \sin \theta |111\rangle, \quad |\psi_{001}\rangle = \cos \theta |001\rangle + \sin \theta |110\rangle, \tag{11}$$

$$|\psi_{010}\rangle = \cos \theta |010\rangle + \sin \theta |101\rangle, \quad |\psi_{011}\rangle = \cos \theta |011\rangle + \sin \theta |100\rangle, \tag{12}$$

$$|\psi_{100}\rangle = \sin \theta |000\rangle - \cos \theta |111\rangle, \quad |\psi_{101}\rangle = \sin \theta |001\rangle - \cos \theta |110\rangle, \tag{13}$$

$$|\psi_{110}\rangle = \sin \theta |010\rangle - \cos \theta |101\rangle, \quad |\psi_{111}\rangle = \sin \theta |011\rangle - \cos \theta |100\rangle. \tag{14}$$

In the same way, we can also define a more general family of entangled W states, given by [32]:

$$|W_1\rangle = \sin \theta \cos \varphi |001\rangle + \sin \theta \sin \varphi |010\rangle + \cos \theta |100\rangle, \tag{15}$$

with $\theta, \varphi \in (0, \pi/2)$. The W state in Equation (8) corresponds to $\varphi = \pi/4$ and $\theta = \cos^{-1}(1/\sqrt{3})$. By using local unitary operations, we can generate the seven other states of the W basis as:

$$|W_2\rangle = + \sin \theta \sin \varphi |001\rangle - \sin \theta \cos \varphi |010\rangle + \cos \theta |111\rangle, \tag{16}$$

$$|W_3\rangle = - \sin \theta \sin \varphi |100\rangle + \cos \theta |010\rangle + \sin \theta \cos \varphi |111\rangle, \tag{17}$$

$$|W_4\rangle = + \sin \theta \cos \varphi |100\rangle + \cos \theta |001\rangle + \sin \theta \sin \varphi |111\rangle, \tag{18}$$

$$|W_5\rangle = + \sin \theta \cos \varphi |110\rangle + \sin \theta \sin \varphi |101\rangle + \cos \theta |011\rangle, \tag{19}$$

$$|W_6\rangle = + \sin \theta \sin \varphi |110\rangle - \sin \theta \cos \varphi |101\rangle + \cos \theta |000\rangle, \tag{20}$$

$$|W_7\rangle = - \sin \theta \sin \varphi |011\rangle + \cos \theta |101\rangle + \sin \theta \cos \varphi |000\rangle, \tag{21}$$

$$|W_8\rangle = + \sin \theta \cos \varphi |011\rangle + \cos \theta |110\rangle + \sin \theta \sin \varphi |000\rangle. \tag{22}$$

⁶ Nevertheless, note that in contrast to the bipartite case, there is no unique way of measuring entanglement in multipartite quantum systems [31].

The state given by Equation (15) can be converted to the maximally entangled W state (Equation (8)) by the process known as entanglement concentration. In [33], efficient schemes for entanglement concentration of an arbitrary W state into a maximally entangled one are presented. In [34], a protocol for entanglement concentration of W states was proposed by using quantum-dot and optical microcavities. A generalization of the protocol mapping arbitrary N-particle less-entangled W states to maximally entangled W states has also been proposed [35]. For additional examples of entanglement concentration protocols, see [36,37].

Now, let us consider the partial trace operation on the third qubit in $|\psi_{000}\rangle$ and $|W_1\rangle$ to examine the differences between the GHZ and W classes. A simple calculation provides:

$$\hat{\rho}_{12} = \text{tr}_3 (|\psi_{000}\rangle\langle\psi_{000}|) = \frac{1}{2} |00\rangle\langle 00| + \frac{1}{2} |11\rangle\langle 11|, \quad (23)$$

for the GHZ state. For the W state, we have:

$$\hat{\rho}_{12} = \text{tr}_3 (|W\rangle\langle W|) = \frac{2}{3} \left| \phi_{01}^{(2)} \right\rangle \left\langle \phi_{01}^{(2)} \right| + \frac{1}{3} |00\rangle\langle 00|. \quad (24)$$

Thus, in the case of a W state, the reduced density operator contains a residual EPR entanglement. In contrast, the same operation on the GHZ state gives a completely disentangled state.

3.2. Other Instances of Tripartite Entanglement

In analogy with the bipartite case, Acín and collaborators, [38], defined a Schmidt-like decomposition useful to classify pure three-qubit states [39]. Subsequently, these results were generalized to include mixed states [40].

In addition to the cases mentioned above, there are several instances of tripartite entanglement. For example, in [41], a procedure to generating a generalization of tripartite GHZ entangled states is presented, using three-level particles instead. In [42], Siewer and Eltschka use the following generalization of the Werner states:

$$\hat{\rho}_W = p |\psi_{000}\rangle\langle\psi_{000}| + \frac{1}{8}(1-p)\hat{1}_8, \quad (25)$$

to treat the problem of entanglement quantification.

3.3. Tripartite Entanglement in Other Areas

It is worth noting that there are several works exploring the idea of entanglement and its classification in other fields in Physics and Mathematics. For instance, there are some works discussing the relationship between entanglement and topology. A connection between Borromean rings and GHZ states was established by Aravind in [43]. In [10], a schematic comparison between GHZ and W tripartite states is presented by using knots. There have been efforts to unveil the relation between quantum entanglement and topological entanglement [44,45]. A recent review on this topic can be found in reference [46]. The idea of entanglement in networks has also been explored.

In [47], a strategy for percolation involving GHZ states was presented. In [48], it was verified experimentally that three and four-party entanglement occurs in quantum networks.

In [49], a connection between black-hole physics and quantum entanglement was demonstrated to exist. This finding shows that there is a match between the classification of tripartite entanglement and black holes. A more recent work concerning this topic is given by reference [50].

In what follows, we present some aspects with regards to three-partite entanglement and foundations of quantum theory. In particular, its relationship with the EPR paradox and Bell inequalities will be described.

4. Non-Locality, Bell’s Theorem and GHZ States

Besides the success of quantum theory describing systems in the microscopic world and all the experimental tests in its favor, the foundations of the theory have been widely discussed since its proposal. Albert Einstein, working with Boris Podolski and Nathan Rosen, for instance, questioned whether quantum mechanics could give a complete description of the physical reality. In a paper published in 1935, they established their famous EPR paradox [15]. In their work, EPR conceived an experiment in which Alice and Bob share an ensemble of entangled pairs of qubits, and each of them can perform local measurements. Under this scenario, the measurement events are separated by space-like intervals. At each instant, Alice may choose one out of two incompatible observables \hat{A}_1 or \hat{A}_2 (analogously for Bob, \hat{B}_1 or \hat{B}_2). Assuming that any local action on each particle cannot influence its counterpart (locality) and that results of the measurement pre-exist for any observable independent of the choice (realism)⁷, they were able to show that two local measurements (one in Alice’s and the other in Bob’s location) allow for determining the values associated with the four involved observables. This finding holds in special systems with a high degree of symmetry and is in contradiction with Heisenberg’s uncertainty principle. EPR concluded that there is no way in which QM satisfies the assumption of local realism and then there should exist a more general theory possibly described by a set of hidden variables (not available to the experimenter). This situation is in analogy with the relationship between thermodynamics and statistical mechanics, in which the position of particles in the phase space play the role of hidden variables. Inspired by this, Bell derived a set of conditions (Bell inequalities) satisfied by predictions from any theory based on local hidden variables, which, as mentioned before, quantum mechanics violates in certain scenarios [51]. Since then many efforts have been made to experimentally test quantum theory against the hypothesis of local realism, with a vast majority in favor of the first one. An important contribution with regards to these experimental tests was reported in 2014. A loophole-free Bell inequality violation was obtained using electron spins separated by 1.3 kilometers [52]. For a recent revision on the subject, we refer the reader to reference [22].

Now, let us analyze the conflict between local realism and the predictions of quantum mechanics by employing a GHZ state. This analysis was initially proposed by Greenberger, Horne and Zeillinger. Here, we present an alternative version by Mermin [53]. For an intuitive introduction, see also [3,54]. An interesting extension which covers W states is given in [55].

First, recall the following relations valid for a single qubit:

$$\hat{\sigma}_x |0\rangle = |1\rangle, \quad \hat{\sigma}_x |1\rangle = |0\rangle, \quad \hat{\sigma}_y |0\rangle = i |1\rangle, \quad \hat{\sigma}_y |1\rangle = -i |0\rangle. \tag{26}$$

Consider three parties, Alice, Bob and Charlie, sharing a state $|\psi_{000}\rangle$ as illustrated in Figure 2. Let us calculate $(\hat{\sigma}_x \otimes \hat{\sigma}_y \otimes \hat{\sigma}_y) |\psi_{000}\rangle$. It means that Alice, Bob, and Charlie apply $\hat{\sigma}_x$, $\hat{\sigma}_y$, and $\hat{\sigma}_y$ locally on their qubits, respectively. This calculation gives:

$$\hat{\sigma}_x \otimes \hat{\sigma}_y \otimes \hat{\sigma}_y |\psi_{000}\rangle = \frac{1}{\sqrt{2}} \hat{\sigma}_x \otimes \hat{\sigma}_y \otimes \hat{\sigma}_y (|000\rangle + |111\rangle) = -1 |\psi_{000}\rangle. \tag{27}$$

Thus, the GHZ state is an eigenstate of $\hat{\sigma}_x \otimes \hat{\sigma}_y \otimes \hat{\sigma}_y$ with eigenvalue -1 . By using the notation employed in [3], we can say that the product:

$$m_x^A m_y^B m_y^C = -1, \tag{28}$$

⁷ The union of both premises is known as the assumption of *local realism*.

where $m_x^A = \pm 1$ indicates the result of the operation $\hat{\sigma}_x$ on Alice’s qubit, for example. We can also calculate $\hat{\sigma}_y \otimes \hat{\sigma}_x \otimes \hat{\sigma}_y |\psi_{000}\rangle$ and $\hat{\sigma}_y \otimes \hat{\sigma}_y \otimes \hat{\sigma}_x |\psi_{000}\rangle$ obtaining the same result, -1 . In this way, we can also write the outcome products as:

$$m_y^A m_x^B m_y^C = -1, \quad m_y^A m_y^B m_x^C = -1. \tag{29}$$

The product of the three terms in Equations (28) and (29) gives

$$m_x^A m_y^B m_y^C m_y^A m_x^B m_y^C m_y^A m_y^B m_x^C = m_x^A m_x^B m_x^C = -1. \tag{30}$$

Please note that in the latter calculations we used the fact that $(m_y^A)^2 = (m_y^B)^2 = (m_y^C)^2 = +1$. Moreover, the calculation of $\hat{\sigma}_x \otimes \hat{\sigma}_x \otimes \hat{\sigma}_x |\psi_{000}\rangle$ leads to a quite different result: $+1 |\psi_{000}\rangle$, which implies that:

$$m_x^A m_x^B m_x^C = +1. \tag{31}$$

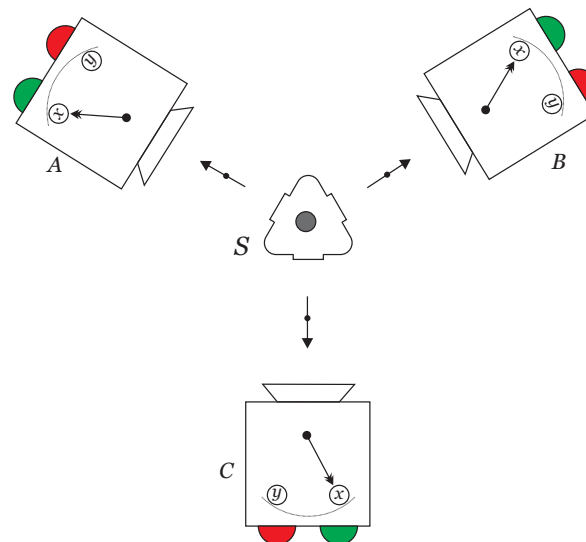


Figure 2. Bell nonlocality in a tripartite scenario. The source S emits three spin-1/2 particles prepared in a GHZ state, traveling to one out of three different detectors located in A, B and C. Each part, namely Alice, Bob and Charlie possess a Stern-Gerlach magnet, and can choose to perform either a $\hat{\sigma}_x$ or a $\hat{\sigma}_y$ measurement, obtaining the eigenvalues $+1$ or -1 , corresponding to turn either green or red lights on.

Thus, there is a contradiction between Equations (30) and (31). It indicates the fundamental impossibility of associating pre-determined outcomes with every local measurement performed on a quantum entangled state. In fact, the so-called GHZ paradox constitutes the first proof of a possible violation of local realism without using an inequality⁸. Furthermore, it is possible to find generalized versions of Bell inequalities for the tripartite case. For instance, Mermin, Ardehali, Belinski, and Klyshko (MABK) independently derived a set of inequalities capable of testing violation of local realism for states of N spin-1/2 particles [57–59]. In addition, Svetlichny made an important contribution to the understanding of genuine tripartite nonlocality [60]. In his work, an inequality that allows for the

⁸ An alternative interesting proof of the violation local realism without using Bell inequalities is given by the Hardy paradox [56].

detection of genuine nonlocality in scenarios involving three observers, each capable of performing one out of two dichotomic measurements, was presented for the first time. In [61], the notion of tripartite entanglement is discussed in contrast to that of nonlocality in the context of the Svetlichny inequality. See also [62] for a definition of genuine multipartite nonlocality that serves as an alternative to Svetlichny’s original proposal. A more recent discussion on tripartite genuine nonlocality can be found in [63].

Tripartite entangled states have been widely used to test the previsions of quantum theory via Models of Local Hidden Variables. For instance, in [64], an experimental test of quantum nonlocality using GHZ states was reported. An experimental setup to generate GHZ states and to test the Svetlichny inequality was also reported [65]. An experimental verification of violations of Mermin’s inequality by distributing tripartite GHZ states between independent observers was achieved [66], closing locality and freedom-of-choice loopholes for three particles. Experimental investigations of nonlocality dealing with W states have also been considered [67]. In [68], an analysis of nonlocality robustness of GHZ and W states under noisy conditions and weak measurements was made. An experimental demonstration of Mermin’s and Svetlichny’s inequalities for GHZ and W states was discussed in [69]. The violation of Svetlichny inequality in the presence of several kinds of noise for the case of GHZ states was studied in [70]. More recently Chaves, Cavalcanti, and Aolita have found new different expressions of nonlocality on tripartite states by using the formalism of Bayesian networks [71].

Several works have been published focusing on the use of both GHZ and W classes as quantum resources to develop quantum protocols, such as quantum teleportation and superdense coding. In fact, as we will see, both classes work in a different way depending on the specific task.

5. Quantum Information Protocols Using Three-Partite Entanglement

Tripartite entanglement can be widely used to execute tasks in the field of quantum information. In this section, we give examples of applicability of this type of entanglement in some protocols.

5.1. Teleportation of a Single-Qubit State by Using a GHZ Channel and EPR Measurements

A scheme to perform quantum teleportation of a qubit state by using a GHZ state as the channel was developed in [72]. In this scheme there are three users, namely Alice, Bob, and Charlie, as shown in Figure 3. They share a GHZ state. Let Alice possess an additional qubit whose state she wants to teleport, $|\phi\rangle = \alpha_0 |0\rangle_1 + \alpha_1 |1\rangle_1$. The state of the system is:

$$|\Psi\rangle = (\alpha_0 |0\rangle + \alpha_1 |1\rangle)_1 \otimes \frac{1}{\sqrt{2}} (|000\rangle + |111\rangle)_{234}. \tag{32}$$

We can write this state in a more compact form as $|\Psi\rangle = \sum_{i=0}^1 \alpha_i |i\rangle_1 \otimes \sum_{j=0}^1 \frac{1}{\sqrt{2}} |jjj\rangle_{234}$. In this case, Alice makes a Bell-measurement on qubits 1 and 2. Let us separate the qubits in the following way:

$$|\Psi\rangle = \frac{1}{\sqrt{2}} \sum_{i,j} \alpha_i |ij\rangle_{12} |jj\rangle_{34}. \tag{33}$$

Let us calculate the projection of $|\Psi\rangle$ into the m, n element of the EPR basis on qubits 1 and 2, $\langle \phi_{mn}^{(2)} |_{12}$. It holds:

$$\langle \phi_{mn} |_{12} |\Psi\rangle = |\eta_{mn}\rangle_{34} = \frac{1}{2} \sum_{ijk} \alpha_i (-1)^{mk} \langle k, k \oplus n | i, j \rangle_{12} \otimes |j, j\rangle_{34} = \sum_{k=0}^1 (-1)^{mk} \alpha_k |k, k \oplus n\rangle_{34}. \tag{34}$$

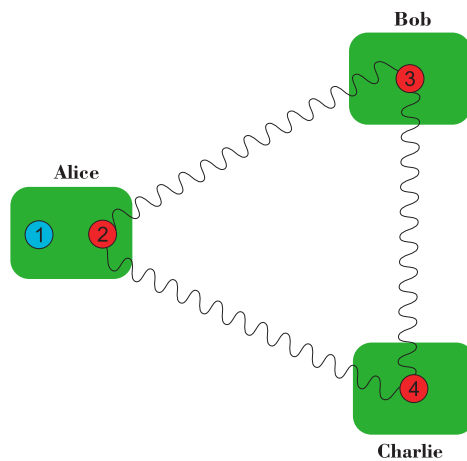


Figure 3. A possible scheme to perform quantum teleportation of a qubit state by using a three-particle entangled state as the quantum channel.

Thus, the state Charlie and Bob share is one out of the four states of the EPR basis (Equation (1), for $d = 2$) and depends on Alice’s measurement result. It is important to note that the new state shared by Charlie and Bob is not a perfect EPR state because the coefficients of this state are α_0 and α_1 . If Alice obtains the state $|\psi_{00}\rangle$, for instance, Bob and Charlie share the state:

$$|\eta_{00}\rangle_{34} = \sum_k \alpha_k |k, k\rangle = \alpha_0 |00\rangle + \alpha_1 |11\rangle. \tag{35}$$

Table 1 exhibits the states that can be shared by Bob and Charlie after Alice’s measurement. Let us explore in more detail the case $|\eta_{00}\rangle$. As shown in [72], to proceed with the protocol, either Bob or Charlie should carry out a measurement on a single qubit. Let us suppose that Alice wants to teleport the state of her input qubit to Charlie. Then, she asks Bob to make a measurement on his part by using the following basis:

$$|0\rangle_3 = \sin \vartheta |x_0\rangle_3 + \cos \vartheta |x_1\rangle_3, \quad |1\rangle_3 = \cos \vartheta |x_0\rangle_3 - \sin \vartheta |x_1\rangle_3. \tag{36}$$

Table 1. Results after Alice’s measurement, labeled by the indexes (m, n) , and corresponding states shared by Bob and Charlie.

Alice’s Result		State Shared by Bob and Charlie
m	n	state
0	0	$ \eta_{00}\rangle = \alpha_0 00\rangle + \alpha_1 11\rangle$
0	1	$ \eta_{01}\rangle = \alpha_0 01\rangle + \alpha_1 10\rangle$
1	0	$ \eta_{10}\rangle = \alpha_0 00\rangle - \alpha_1 11\rangle$
1	1	$ \eta_{11}\rangle = \alpha_0 01\rangle - \alpha_1 10\rangle$

After carrying out proper substitutions in Equation (35), we have:

$$|\eta_{00}\rangle_{34} = \alpha_0 (\sin \vartheta |x_1\rangle_3 + \cos \vartheta |x_2\rangle_3) |0\rangle_4 + \alpha_1 (\cos \vartheta |x_1\rangle_3 - \sin \vartheta |x_2\rangle_3) |0\rangle_4. \tag{37}$$

We can reorganize this expression as:

$$|\eta_{00}\rangle_{34} = |x_1\rangle_3 (\alpha_0 \sin \vartheta |0\rangle_4 + \alpha_1 \cos \vartheta |1\rangle_4) + |x_2\rangle_3 (\alpha_0 \cos \vartheta |0\rangle_4 - \alpha_1 \sin \vartheta |1\rangle_4). \tag{38}$$

Thus, if Bob’s measurement outcome is $|x_1\rangle$, then the state of Charlie’s qubit (up to normalization) is projected onto $\alpha_0 \sin \vartheta |0\rangle_4 + \alpha_1 \cos \vartheta |1\rangle_4$. Table 1 shows all possibilities after subsequent measurements by Alice and Bob.

Let us come back to the general case by defining $b_0 \equiv \sin \vartheta$ and $b_1 \equiv \cos \vartheta$. We can then write Bob’s measurement basis as:

$$|k\rangle_3 = \sum_{j=0}^1 (-1)^{jk} b_{j\oplus k} |x_j\rangle_3. \tag{39}$$

In this way we have:

$$|\eta_{mn}\rangle_{34} = \sum_{k=0}^1 (-1)^{mk} \alpha_k \left(\sum_{j=0}^1 (-1)^{jk} b_{j\oplus k} |x_j\rangle_3 \right) |k \oplus n\rangle_4. \tag{40}$$

To obtain the final state of Charlie’s qubit, we can calculate the projection of the above state on $|x_j\rangle$, where $j = 0, 1$.

$$|\chi_{mnj}\rangle_4 = \langle x_j |_3 |\eta_{mn}\rangle_{34} = \sum_{k=0}^1 (-1)^{(m\oplus j)k} \alpha_k b_{k\oplus j} |k \oplus n\rangle. \tag{41}$$

The indexes (m, n, j) are related to the measurement outcomes on Alice and Bob parts. A complete list of the correspondence between outcomes and final states for Charlie is presented in Table 2. To recover the desired state, Charlie needs to apply a unitary transformation on his qubit. Which unitary transformation he will choose depends on Alice’s and Bob’s measurement outcomes. Table 3 shows a list of operations for all results. For instance, for the case $(0, 0, 0)$, the state (up to normalization) is:

$$|\chi_{000}\rangle = \alpha_0 \sin \vartheta |0\rangle_4 + \alpha_1 \cos \vartheta |1\rangle_4. \tag{42}$$

Table 2. Alice’s and Bob’s measurement outcomes and corresponding projected states in Charlie’s location.

Alice’s Result	Bob’s Result	Charlie’s Unnormalized State
m	n	State
0	0	$\alpha_0 \sin \vartheta 0\rangle + \alpha_1 \cos \vartheta 1\rangle$
0	0	$\alpha_0 \cos \vartheta 0\rangle - \alpha_1 \sin \vartheta 1\rangle$
0	1	$\alpha_0 \sin \vartheta 1\rangle + \alpha_1 \cos \vartheta 0\rangle$
0	1	$\alpha_0 \cos \vartheta 1\rangle - \alpha_1 \sin \vartheta 0\rangle$
1	0	$\alpha_0 \sin \vartheta 0\rangle - \alpha_1 \cos \vartheta 1\rangle$
1	0	$\alpha_0 \cos \vartheta 0\rangle + \alpha_1 \sin \vartheta 1\rangle$
1	1	$\alpha_0 \sin \vartheta 1\rangle - \alpha_1 \cos \vartheta 0\rangle$
1	1	$\alpha_0 \cos \vartheta 1\rangle + \alpha_1 \sin \vartheta 0\rangle$

In this case, the required operation is the identity. The normalized state reads:

$$|\zeta_{000}\rangle_f = \frac{\alpha_0 \sin \vartheta |0\rangle_4 + \alpha_1 \cos \vartheta |1\rangle_4}{\sqrt{|\alpha_0|^2 \sin^2 \vartheta + |\alpha_1|^2 \cos^2 \vartheta}}. \tag{43}$$

Let us see what happens when the result is $(0, 0, 1)$. In this case, the state, up to normalization, is:

$$|\chi_{001}\rangle = \alpha_0 \cos \vartheta |0\rangle_4 - \alpha_1 \sin \vartheta |1\rangle_4; \tag{44}$$

now, Charlie must apply the $\hat{\sigma}_z$ operation on his qubit to recover the desired state. After normalization, we have:

$$|\zeta_{001}\rangle_f = \frac{\alpha_0 \cos \vartheta |0\rangle_4 + \alpha_1 \sin \vartheta |1\rangle_4}{\sqrt{|\alpha_0|^2 \cos^2 \vartheta + |\alpha_1|^2 \sin^2 \vartheta}}. \tag{45}$$

Explicitly, the unitary transformation is given by:

$$\hat{U} = (\hat{\sigma}_z)^{m\oplus j} (\hat{\sigma}_x)^n. \tag{46}$$

Thus, the final state is:

$$\hat{U} |\chi_{mnj}\rangle = |\zeta_{mnj}\rangle = \sum_k \alpha_k b_{k\oplus j} |k\rangle. \tag{47}$$

Then, Charlie’s qubit holds in the same state as the initial one whenever $\theta = \pi/4$, i.e., Bob’s measurement is carried out in the $|\pm\rangle$ basis. Another work dealing with GHZ states as the quantum channel can be found in [73].

Table 3. Alice’s and Bob’s results; and the corresponding operations needed to recover the desired state.

Result: (m, n, i)	Operation
(0, 0, 0)	\hat{I}
(0, 0, 1)	$\hat{\sigma}_z$
(0, 1, 0)	$\hat{\sigma}_x$
(0, 1, 1)	$\hat{\sigma}_z \hat{\sigma}_x$
(1, 0, 0)	$\hat{\sigma}_z$
(1, 0, 1)	\hat{I}
(1, 1, 0)	$\hat{\sigma}_z \hat{\sigma}_x$
(1, 1, 1)	$\hat{\sigma}_x$

5.2. Teleportation of a Single-Qubit State: GHZ Channel and Measurement

Another possibility of using GHZ states in quantum teleportation is by employing a GHZ channel and making a GHZ measurement on Alice’s side. An example of a protocol dealing with GHZ measurements can be viewed in [74]. Let us suppose that now Alice wants to teleport a single qubit and shares a GHZ entangled state with Bob. We want to consider the situation that Alice shares two qubits of the shared GHZ state and that Bob has another one. Thus, now Alice has three qubits and Bob has one. To diversify the mathematical approach used here, we intend to write the states by using the formalism of the density matrix. This problem has been discussed in [75] where a maximally balanced state as the channel and measurements was considered. This procedure was shown to help to improve the quality of the protocol under the occurrence of bit-flip errors. Here, let us consider non-maximally entangled GHZ states. It is interesting to take into account such states, because we can study how the quality of the entanglement affects the final results. The effect of dealing with non-maximally GHZ entangled states can also be examined in other scenarios. In [76], for instance, the problem of sharing a multiqubit state by employing non-maximally GHZ entangled states is addressed.

Consider the scheme of Figure 4. Alice wants to teleport the state of qubit 1:

$$|\phi\rangle_1 = \alpha_0 |0\rangle_1 + \alpha_1 |1\rangle_1 = \sum_{i=0}^1 \alpha_i |i\rangle_1. \tag{48}$$

The corresponding density operator is given by:

$$\hat{\rho}_1 = \sum_{ij} \alpha_i \alpha_j^* |i\rangle \langle j|. \tag{49}$$

The channel is a GHZ-type state of the qubits 2, 3, 4, expressed in the form $|\psi_{001}\rangle = \beta_0 |000\rangle + \beta_1 |111\rangle$, where $\beta_0 = \cos \theta$ and $\beta_1 = \sin \theta$. We can write this state as $|\psi_{001}\rangle_{ghz} = \sum_{k=0}^1 \beta_k |kkk\rangle$.

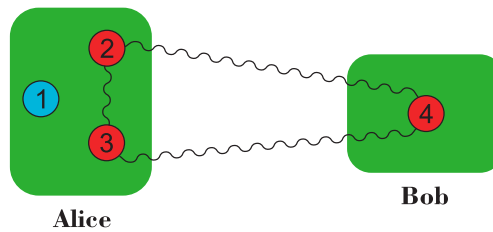


Figure 4. Scheme to teleport a single-qubit state by using a GHZ state as the quantum channel. A GHZ measurement is carried out on qubits 1, 2, 3.

The corresponding density operator of the whole system is:

$$\hat{\rho}_{234} = \sum_{k\ell} \beta_k \beta_\ell |kkk\rangle \langle \ell\ell\ell|. \tag{50}$$

The state of the whole system reads:

$$\hat{\rho} = \hat{\rho}_1 \otimes \hat{\rho}_{234} = \sum_{ijkl} \alpha_i \alpha_j^* \beta_k \beta_\ell |ikkk\rangle_{1234} \langle j\ell\ell\ell|_{1234}. \tag{51}$$

Let us separate the qubits that will be part of the GHZ measurement:

$$\hat{\rho} = \hat{\rho}_1 \otimes \hat{\rho}_{234} = \sum_{ijkl} \alpha_i \alpha_j^* \beta_k \beta_\ell |ikk\rangle_{123} \langle j\ell\ell|_{123} \otimes |k\rangle_4 \langle \ell|_4. \tag{52}$$

To perform the measurement, we will consider the basis introduced in Equation (10). After the measurement, the unnormalized state is given by:

$$\tilde{\rho}_I(\mu, \lambda, \omega) = \sum_{j'k'} (-1)^{\mu j'} (-1)^{\mu k'} b_{\mu \oplus j'} b_{\mu \oplus k'} \beta_{k' \oplus \lambda} \beta_{j' \oplus \lambda} \delta_{\lambda, \omega} \alpha_{k'} \alpha_{j'}^* |k' \oplus \lambda\rangle_4 \langle j' \oplus \lambda|_4. \tag{53}$$

This state depends on the parameters related to the measurement, (μ, λ, ω) . For the case where, for example, $(\mu, \lambda, \omega) = (0, 0, 0)$ we have:

$$\tilde{\rho}_I(0, 0, 0) = \sum_{j'k'} (b_{j'} b_{k'} \beta_{j'} \beta_{k'} \delta_{\lambda, \omega}) \alpha_{k'} \alpha_{j'}^* |k'\rangle \langle j'|. \tag{54}$$

More explicitly:

$$\tilde{\rho}_I(0, 0, 0) = b_0^2 \beta_0^2 |\alpha_0|^2 |0\rangle \langle 0| + b_1^2 \beta_1^2 |\alpha_1|^2 |1\rangle \langle 1| + b_0 b_1 \beta_0 \beta_1 (\alpha_0 \alpha_1^* |0\rangle \langle 1| + \alpha_1 \alpha_0^* |1\rangle \langle 0|). \tag{55}$$

On the other hand:

$$\tilde{\rho}_I(1, 1, 1) = \sum_{j'k'} (-1)^{j'} (-1)^{k'} b_{j' \oplus 1} b_{k' \oplus 1} \beta_{k' \oplus 1} \beta_{j' \oplus 1} \delta_{\lambda, \omega} \alpha_{k'} \alpha_{j'}^* |k' \oplus 1\rangle_4 \langle j' \oplus 1|_4, \tag{56}$$

or:

$$\tilde{\rho}_I(1, 1, 1) = b_1^2 \beta_1^2 |\alpha_0|^2 |1\rangle \langle 1| + b_0^2 \beta_0^2 |\alpha_1|^2 |0\rangle \langle 0| - b_0 b_1 \beta_0 \beta_1 (\alpha_1 \alpha_0^* |0\rangle \langle 1| + \alpha_0 \alpha_1^* |1\rangle \langle 0|). \tag{57}$$

The normalized state after the measurement is given by:

$$\hat{\rho}_I = \hat{\rho}_I(\mu, \lambda, \omega) = \frac{\hat{P} \hat{\rho}_0 \hat{P}^\dagger}{P} = \frac{\tilde{\rho}_I}{P}, \tag{58}$$

where:

$$\hat{P} = \hat{P}_{\mu\lambda\omega} = |\Phi_{\lambda}^{\mu}\rangle\langle\Phi_{\lambda\omega}^{\mu}|_{123} \tag{59}$$

is the projector associated with the GHZ measurement and:

$$P = P_{\mu\lambda\delta\omega} = Tr(\hat{P}\hat{\rho}_0) \tag{60}$$

corresponds to probability of each outcome.

Each outcome (μ, λ, ω) requires a unitary transformation to recover the desired state. In the case $(0, 0, 0)$, the operation is just the identity. In the case $(1, 1, 1)$, Bob needs to apply $\hat{\sigma}_z\hat{\sigma}_x$. Looking at the expression of $\tilde{\rho}_I$, it is possible to suggest that the general form of the operation needed is given by:

$$\hat{U} = \hat{U}_{\mu\lambda\omega} = (\hat{\sigma}_z)^{\mu}(\hat{\sigma}_x)^{\lambda}. \tag{61}$$

After the measurement, by using a classical channel, Alice informs Bob which μ and λ are needed to recover the desired state. We can check if this operation works by calculating $\hat{U}\tilde{\rho}_I\hat{U}^{\dagger}$.

$$\tilde{\rho}_f = \hat{U}\tilde{\rho}_I\hat{U}^{\dagger} = \sum_{j'k'} b_{\mu\oplus j'} b_{\mu\oplus k'} \beta_{k'\oplus\lambda} \beta_{j'\oplus\lambda} \delta_{\lambda,\omega} \alpha_{k'} \alpha_{j'}^* |k'\rangle\langle j'|. \tag{62}$$

In this way, the unitary transformation corrects the factor $k' \oplus \lambda$ on the ket as well as the factor $(-1)^{\mu k'}$. However, it is impossible to correct the factors involving b and β . The fidelity corresponding to a specific outcome is:

$$F_{\mu\lambda\omega} = Tr(\hat{\rho}_{in}\tilde{\rho}_f). \tag{63}$$

The average fidelity reads:

$$\bar{F} = \sum_{\mu\lambda\omega} P_{\mu\lambda\omega} F_{\mu\lambda\omega} = \sum_{\mu\lambda\omega} P_{\mu\lambda\omega} Tr[\hat{\rho}_{in}\tilde{\rho}_f]. \tag{64}$$

Here, ρ_f is the final state after the unitary transformation. When we deal with GHZ maximally entangled states, we know that the probability of obtaining a specific outcome is the same of the others (the probability is the same for all outcomes). It is not true in more general cases. Then, this average fidelity takes into account that when we deal with non-maximally entangled states, the probability of obtaining an outcome depends on the amount of entanglement. Also, each outcome has a different probability. In this case, we need to sum all the contributions of each outcome times the corresponding statistical weight $P_{\mu\lambda\omega}$. But:

$$\hat{\rho}_f = \frac{\hat{U}\tilde{\rho}_I\hat{U}^{\dagger}}{P_{\mu\lambda\omega}} = \frac{\tilde{\rho}_f}{P_{\mu\lambda\omega}}. \tag{65}$$

Thus:

$$\bar{F} = \sum_{\mu\lambda\omega} Tr[\hat{\rho}_{in}\tilde{\rho}_f], \tag{66}$$

or:

$$\bar{F} = \sum_{k\ell\mu\nu\lambda\omega} |\alpha_k|^2 |\alpha_{\ell}|^2 b_{\mu\oplus k}^* b_{\mu\oplus\ell} \beta_{k\oplus\lambda} \beta_{\ell\oplus\lambda}. \tag{67}$$

Performing all the sums, we have:

$$\bar{F} = |\alpha_0|^4 + |\alpha_1|^4 + 2|\alpha_0|^2 |\alpha_1|^2 (b_0 b_1 \beta_0 \beta_1). \tag{68}$$

The expression above depends on the initial state. To obtain a quantity independent of the parameters of the initial state, let us consider that the initial state can be parametrized as:

$$|\Psi\rangle_{in} = |\alpha_0\rangle|000\rangle + |\alpha_1\rangle e^{i\varphi} |111\rangle. \tag{69}$$

In such a way, we can now calculate an average of all possible input states:

$$\langle \bar{F} \rangle = \frac{1}{2\pi} \int_0^{2\pi} \int_0^1 \bar{F}(|\alpha_0|^2, \varphi) d|\alpha_0|^2 d\varphi. \tag{70}$$

Evaluating the integral, we obtain:

$$\langle \bar{F} \rangle = \frac{2}{3} + \frac{1}{3} \sin(2\theta) \sin(2\phi). \tag{71}$$

In this expression, the first term corresponds to the classical contribution, and the second one depends on the entanglement of the channel and measurement basis. Essentially, it has the same form as the fidelity for the standard teleportation protocol, using EPR channel and measurements. However, as pointed out in [75], in the presence of bit-flip noise, GHZ states allow for corrections of this kind of errors. In this way, it is possible to improve fidelity.

In Figure 5, we plot the fidelity as a function of θ and ϕ . When the states on the channel and in the measurement basis are maximally entangled, the maximum fidelity is reached, corresponding to $\langle \bar{F} \rangle = 1$, which is the ideal case.

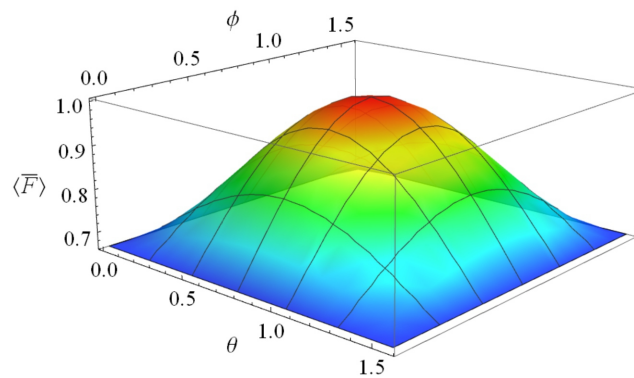


Figure 5. Fidelity of teleportation corresponding to the case of a single-qubit state by using a GHZ channel as a function of the entanglement parameters in the channel and measurement basis. Please note that the maximum fidelity is obtained whenever $\theta = \phi = \pi/4$, i.e., for maximum entanglement.

5.3. Teleportation of a Two-Qubit State

A very interesting proposal involves the teleportation of a two-qubit entangled state [77]. An EPR-like state, for example, can be teleported by using GHZ states as the channel [78]. Other schemes have also been proposed [79,80]. Recently, a scheme to teleport an arbitrary two-qubit state by using two GHZ states [81] was presented. In [82], a protocol to teleport a two-qubit state by using both GHZ and W states simultaneously as the quantum channel was developed. Teleportation of an EPR state by a non-maximally entangled GHZ quantum channel is also possible [83]. In [84], a scheme to perform bidirectional teleportation of an EPR state by employing GHZ states was shown. In [85], a protocol dealing with a composite channel using EPR and GHZ states to execute a multihop teleportation of a two-qubit state is presented. In reference [86], a scheme is introduced to teleport an arbitrary two-qubit state based on a channel consisting of a tripartite entangled state (GHZ or W) and an EPR state.

Figure 6 shows a possible scheme to teleport an EPR state. A GHZ state can be used as the quantum channel, and a measurement in a GHZ basis on the qubits 1, 2, and 3 is performed. The state of the system is:

$$(\alpha_0 |00\rangle + \alpha_1 |11\rangle)_{12} \otimes \frac{1}{\sqrt{2}}(|000\rangle + |111\rangle)_{345}. \tag{72}$$

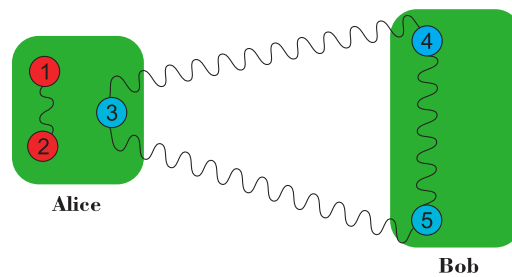


Figure 6. An EPR state can be teleported by using a GHZ state as the quantum channel. In this case, a measurement in the GHZ basis is also necessary.

5.4. Teleportation of a GHZ State

Another possibility of a quantum teleportation protocol is the teleportation of a GHZ state. This is an interesting aspect, because besides performing teleportation of information itself, the protocol also provides a way of delivering quantum entanglement to initially distant locations. It is relevant in the sense that the distribution of entanglement could be used, in principle, to connect several distant users in a quantum network, for example. Several works have addressed this problem. In [87], the teleportation of a GHZ state with N photons by using a two-photon entangled state as the quantum channel was investigated. A scheme to teleport a GHZ state via entanglement-swapping is shown in [88]. The teleportation of a GHZ state by using two W entangled states as the quantum channel was considered in [89]. GHZ states can also be transmitted through a multihop teleportation scheme by using Bell’s states as intermediate quantum channels [90]. In [91], a scheme to teleport a GHZ-like state by employing three pairs of non-maximally entangled states as the quantum channel was proposed. The configuration to make the protocol is illustrated in Figure 7. In [92], a similar protocol to the latter was presented, but this time it was designed to teleport an arbitrary tripartite state.

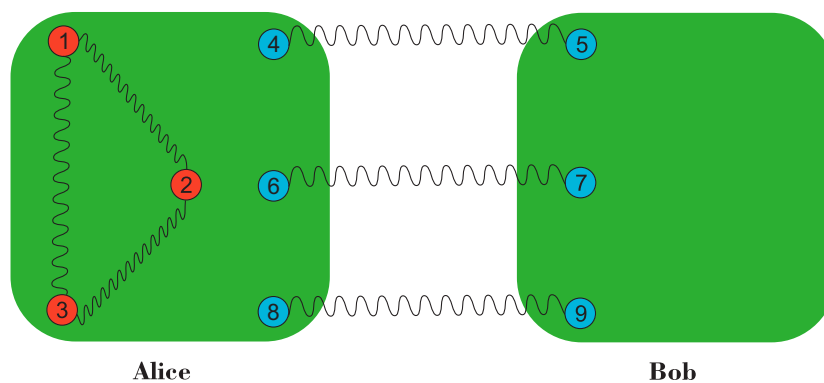


Figure 7. Scheme to teleport a GHZ state. In this scheme, three EPR states are used as the quantum channel and EPR measurements are taken on qubits 1, 4 and 2, 6 and 3, 8, respectively. At the end, the qubits 5, 7, 9 hold in a GHZ state.

Figure 7 shows a possible scheme to develop a teleportation protocol of a GHZ state by using three EPR states as the quantum channel. The state of the system is given by:

$$|\Psi\rangle = |\phi\rangle_{123} \otimes |\eta\rangle_{45} \otimes |\chi\rangle_{67} \otimes |\zeta\rangle_{89}, \tag{73}$$

where:

$$|\phi\rangle_{123} = \alpha_0 |000\rangle_{123} + \alpha_1 |111\rangle_{123}, \tag{74}$$

$$|\eta\rangle_{45} = \sum_j b_j |jj\rangle_{45}, \quad |\chi\rangle_{67} = \sum_k c_k |kk\rangle_{67}, \quad |\zeta\rangle_{89} = \sum_\ell x_\ell |\ell\ell\rangle_{89}. \tag{75}$$

In this scheme, Alice makes three EPR measurements on her side. The measurements are taken on particles (1, 4), (2, 6) and (3, 8). Reference [91] shows the procedure in detail to finish the protocol.

5.5. Teleportation of a Single-Qubit State Using a W Channel

In [93], a possible scheme to deal with a single-qubit state teleportation by employing a W state as the channel and an EPR measurement was reported, showing that W states are suitable to make the protocol in a probabilistic manner. In that work, some calculations of probabilities were erroneous. Subsequently, the errors were corrected by [94] and [95]. However, although the conclusion presented in [93] is correct, the calculations for the case of a W state with the generic state is not quite precise. As follows, we explicitly perform the calculations for the teleportation of a qubit state by using a generic W state. The state to be teleported is:

$$|\phi\rangle_1 = \alpha_0 |0\rangle_1 + \alpha_1 |1\rangle_1. \tag{76}$$

The channel is given by:

$$|W\rangle_{234} = a |100\rangle_{234} + b |010\rangle_{234} + c |001\rangle_{234}. \tag{77}$$

The general state of the system reads:

$$|\Psi\rangle = [\alpha_0 |0\rangle + \alpha_1 |1\rangle]_1 \otimes [a |100\rangle + b |010\rangle + c |001\rangle]_{234}. \tag{78}$$

More explicitly, we have:

$$|\Psi\rangle = \alpha_0 a |0100\rangle_{1234} + \alpha_0 b |0010\rangle_{1234} + \alpha_0 c |0001\rangle_{1234} + \alpha_1 a |1100\rangle_{1234} + \alpha_1 b |1010\rangle_{1234} + \alpha_1 c |1001\rangle_{1234}. \tag{79}$$

Now, we can write the states of qubits 1 and 2 in terms of the EPR basis.

$$\begin{aligned} |\Psi\rangle = & \frac{\alpha_0 a}{\sqrt{2}} (|\psi^+\rangle + |\psi^-\rangle)_{12} |00\rangle_{34} + \frac{\alpha_0 b}{\sqrt{2}} (|\Phi^+\rangle + |\Phi^-\rangle)_{12} |10\rangle_{34} \\ & + \frac{\alpha_0 c}{\sqrt{2}} (|\Phi^+\rangle + |\Phi^-\rangle)_{12} |01\rangle_{34} + \frac{\alpha_1 a}{\sqrt{2}} (|\Phi^+\rangle - |\Phi^-\rangle)_{12} |00\rangle_{34} \\ & + \frac{\alpha_1 b}{\sqrt{2}} (|\psi^+\rangle - |\psi^-\rangle)_{12} |10\rangle_{34} + \frac{\alpha_1 c}{\sqrt{2}} (|\psi^+\rangle - |\psi^-\rangle)_{12} |01\rangle_{34}; \end{aligned} \tag{80}$$

We can write this expression in the following way:

$$\begin{aligned} |\Psi\rangle = & \frac{|\Phi^+\rangle_{12}}{\sqrt{2}} [\alpha_0 b |10\rangle + \alpha_0 c |01\rangle + \alpha_1 a |00\rangle]_{34} + \frac{|\Phi^-\rangle_{12}}{\sqrt{2}} [\alpha_0 b |10\rangle + \alpha_0 c |01\rangle - \alpha_1 a |00\rangle]_{34} \\ & + \frac{|\psi^+\rangle_{12}}{\sqrt{2}} [\alpha_0 a |00\rangle + \alpha_1 b |10\rangle + \alpha_1 c |01\rangle]_{34} + \frac{|\psi^-\rangle_{12}}{\sqrt{2}} [\alpha_0 a |00\rangle - \alpha_1 b |10\rangle - \alpha_1 c |01\rangle]_{34}. \end{aligned} \tag{81}$$

Separating the qubits 3 and 4 results in:

$$\begin{aligned}
 |\Psi\rangle = & \frac{|\Phi^+\rangle_{12}}{\sqrt{2}} \left[\left(\alpha_0 b |1\rangle_3 + \alpha_1 a |0\rangle_3 \right) |0\rangle_4 + \alpha_0 c |0\rangle_3 |1\rangle_4 \right] \\
 & + \frac{|\Phi^-\rangle_{12}}{\sqrt{2}} \left[\left(\alpha_0 b |1\rangle_3 - \alpha_1 a |0\rangle_3 \right) |0\rangle_4 + \alpha_0 c |0\rangle_3 |1\rangle_4 \right] \\
 & + \frac{|\psi^+\rangle_{12}}{\sqrt{2}} \left[\left(\alpha_0 a |0\rangle_3 + \alpha_1 b |1\rangle_3 \right) |0\rangle_4 + \alpha_1 c |0\rangle_3 |1\rangle_4 \right] \\
 & + \frac{|\psi^-\rangle_{12}}{\sqrt{2}} \left[\left(\alpha_0 a |0\rangle_3 - \alpha_1 b |1\rangle_3 \right) |0\rangle_4 - \alpha_1 c |0\rangle_3 |1\rangle_4 \right]. \tag{82}
 \end{aligned}$$

Let us suppose that after a measurement on qubits 1 and 2 in the EPR basis, Alice obtains $|\psi^+\rangle$. In this case, the unnormalized state of qubits 3 and 4 is given by:

$$\frac{1}{\sqrt{2}} \left[\left(\alpha_0 a |0\rangle_3 + \alpha_1 b |1\rangle_3 \right) |0\rangle_4 + \alpha_1 c |0\rangle_3 |1\rangle_4 \right]. \tag{83}$$

It is worth noting that the joint state of the qubits 3 and 4 also contains EPR entanglement. In this way, after a single-qubit measurement, it is possible to complete the protocol. If the qubit 4 is projected on the $|0\rangle$ state, then the state of qubit 3 (up to normalization) will be $|\eta\rangle_3 = \alpha_0 a |0\rangle_3 + \alpha_1 b |1\rangle_3$. This state looks like the initial state $|\phi\rangle_1$. However, there is an imperfection due the coefficients a and b . We can say that the initial state was teleported, but contained an imperfection. On the other hand, if the qubit 4 is projected on the state $|1\rangle$, teleportation does not occur. In this way, we can conclude that the protocol works probabilistically. A further paper on the use of W states as the quantum channel is stated in [96]. In [97], the teleportation of a single-qubit state was also analyzed. After that, an important contribution was provided by [98] where it was shown that there is a type of W state that can be used for perfect teleportation and superdense coding. This work was generalized in [99]. In [100], a composite W-Bell channel is used to execute quantum teleportation and superdense coding protocols.

5.6. Teleportation of a W State

A quantum teleportation scheme of a tripartite W state was presented in [101]. In that scheme, shown in Figure 8, Alice wants to teleport the state,

$$|\phi\rangle_{123} = \alpha_0 |001\rangle_{123} + \alpha_1 |010\rangle_{123} + \alpha_2 |100\rangle_{123}, \tag{84}$$

on particles 1, 2, 3. She shares two entangled states with Bob, a GHZ state, and an EPR state, which will be used as the quantum channels. The EPR state is given by:

$$|\psi\rangle_{45} = a_0 |00\rangle_{45} + a_1 |11\rangle_{45}, \tag{85}$$

and the GHZ state is:

$$|\eta\rangle_{678} = \beta_0 |000\rangle_{678} + \beta_1 |111\rangle_{678}. \tag{86}$$

The state of the whole system reads:

$$|\Psi\rangle = |\phi\rangle_{123} \otimes |\psi\rangle_{45} \otimes |\eta\rangle_{678}. \tag{87}$$

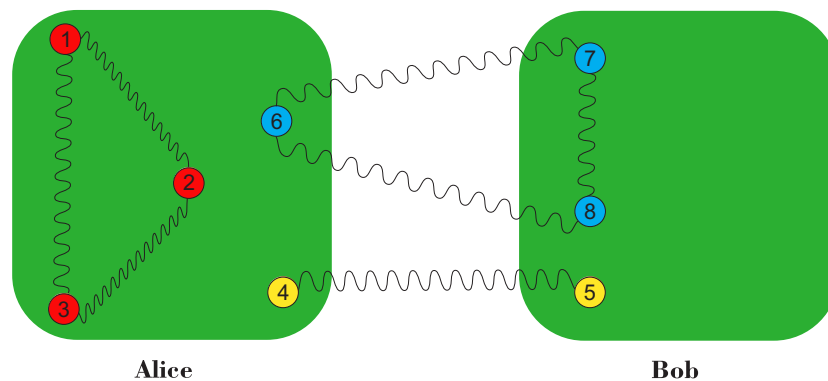


Figure 8. A possible way of teleporting a W state is illustrated. A GHZ state and an EPR channel are used as the quantum channel.

Particles 1, 2, 3, 4, and 6 are on Alice's side, while particles 5, 7, and 8 are on Bob's side. To execute the teleportation, two EPR measurements are taken on particles 1, 6 and 3, 4. After the measurements, the resultant state involves particles 2, 5, 7, and 8. Thus, it is necessary to trace out particle 2. Here, the protocol is more complicated than that discussed previously. Now, it is necessary to employ combinations of a Hadamard gate and a CNOT gate as well as to introduce an auxiliary particle. All procedures to carry out are presented in reference [101]. More recently, another scheme to teleport a W state was provided by reference [102] where two W states are used as the quantum channel.

5.7. Dense Coding

The original Dense Coding was presented by using a two-entangled state as the resource, but tripartite entanglement is also suitable to make the protocol work [103]. Several schemes have been proposed to do so. Two examples of controlled dense coding dealing with GHZ states can be accessed in [104,105]. The W state is also suitable to make a controlled dense coding protocol [106]. Super Dense Coding with W states was studied recently in [107]. In [108], a scheme was proposed to implement a dense coding protocol by employing tripartite entanglement in cavity QED. In [109] the use of GHZ and W states to make Deterministic Dense Coding was analyzed.

5.8. Quantum Cryptography and Quantum Secure Communication

Quantum Mechanics can also be used to perform cryptographic protocols. The base of this field was founded by Wiesner [110]. Subsequently, other fundamental steps were due to C. Bennet and G. Brassard (scheme known as BB84 protocol) [111], and A. Ekert [112]. After these initial developments, the use of multipartite entanglement has been considered. In [113], it was shown that a GHZ state can be used to make the quantum secret sharing protocol. In [114], some variants of protocols of quantum secure communication dealing with W states were presented.

Schemes to establish a three-party quantum secure communication using GHZ states are provided in [115,116]. In [117], a protocol is proposed for quantum secure direct communication using W states. Secure quantum protocols also have been studied in the framework of Measurement Device Independence (MDI). In [118], for instance, a MDI Quantum Key Distribution (QKD) scheme was developed that can work by using standard optical components with low detection efficiency and highly lossy channels. The technology employed in MDI-QKD can be used to perform long-distance MDI multiparty communication. In [119], this idea was employed to propose a feasible scheme for distributing post-selected GHZ entanglement over a distance of more than 100 km in an experimentally relevant parameter regime.

5.9. Other Developments

In [120], a quantum protocol to send and receive messages anonymously was presented where n players have access to a shared n -qubit GHZ entangled state. Recently, a scheme to transmit an anonymous message in a network employing W -type states with N qubits [121] was developed. In [122], quantum algorithms to the generation of GHZ and W states of n qubits are proposed to be used on quantum networks. In [123], tripartite entanglement in a non-inertial frame with one of the parties subject to a uniform acceleration is examined. Tripartite entanglement also has been studied in the context of distillation of entanglement.

Methods of distillation of GHZ states can be accessed in [124,125]. Protocols for the optimal distillation of W states were given in [126]. In [127], a method for entanglement purification of three-qubit states by using weak measurements is presented. In [128], a distillation of GHZ-type states from two copies of a mixed state in a single step was shown.

The relationship between tripartite entanglement and quantum computing can also be explored. In [129], it was demonstrated that a GHZ state can be used as an ingredient in the construction of a universal quantum computer. The relationship between state complexity and quantum computing is discussed in [130], including GHZ and W states in the analysis. A discussion on the computational power of GHZ and W states is provided in [131]. In [132], a conceptual design for a quantum block-chain by using a temporal entangled GHZ state was proposed.

6. Production of Three-Partite Entanglement

The production of multipartite entanglement has attracted much attention. An experimental demonstration of five-qubit entanglement was realized by Zhao and collaborators [133] in 2004. In 2011, Huang and colleagues reported an experimental realization of an eight-photon Greenberger—Horne—Zeilinger state. In the same year, the creation of an entangled state of 14 qubits was also presented [134]. The first experimental production of a three-photon GHZ state was reported in 1999 [135]. Since then, several works have been proposed, employing different frameworks. Recently, the deterministic generation of an 18-qubit entangled GHZ state was achieved. An experimental realization of a W state was reported in [136]. In [137], a pioneer scheme for generating three-particle entanglement was introduced by using just two pairs of entangled particles from independent emissions. Another pioneer work involving GHZ states is by Bouwmeester and colleagues [135], observing the GHZ entanglement for three qubits in the polarization degree of freedom of photons. The creation of maximally entangled GHZ states by using Nuclear Magnetic Resonance (NMR) is also possible [138]. A proposal for a creation of GHZ and W states via quantum walks can be accessed in [139]. Multipartite entanglement can also be generated by using a single-neutron interferometer [140]. In [141], a scheme was proposed to prepare a W state using parametric down-conversion. Schemes to prepare GHZ and W states of three distant atoms were provided in [142]. A method to generate an n -qubit W state in cavity QED was reported in [143]. In [144], a scheme to generating W states from atomic ensembles is presented. The creation of GHZ and W states with a trapped-ion quantum computer was reported in [145]. The preparation of spin-qubit GHZ and W states in a quantum-dot-microcavity system was discussed in [146]. It is also possible to generate W states of three superconducting qubits [147]. A scheme to generate entanglement between three atoms trapped in cavities via quantum Zeno dynamics was proposed in [148]. In [149], we can encounter a scheme to generate GHZ and W states from cavities with Jaynes—Cummings Hamiltonians. In [150], a procedure to creating three-photon polarization entanglement was shown and the characterization of the produced states was made. Such states are used to test local realism. Recently, a scheme to generate GHZ states encoded in the path degree of freedom of three photons was presented in [151]. Another recent proposal for the generation of tripartite entanglement can be accessed in [152] where the creation of W states employing cross-Kerr nonlinearity and quantum dots is addressed. The production of larger states involving multi-qubits is desirable to make protocols involving quantum networks [48]. Several steps have been achieved in this direction. For example, A scalable scheme to create W states

was presented in 2017 [153]. In [154], a deterministic scheme for preparing W states of size of any power of 2 was presented. Recently, a scheme to prepare an N -qubit GHZ state in a chain of four-level Rydberg atoms was proposed in [155]. In [156], the creation of entangled states with up to 20 qubits was demonstrated.

7. Detection and Characterization of Tripartite Entanglement

The detection of multipartite entanglement is a hard task [157]. Several efforts, both theoretical and experimental ones, have been made to improve the methods to do so. The detection of entanglement involves a key ingredient: the construction of Entanglement Witness [158,159]. In several practical situations, it is possible to certify entanglement through the violation of some inequality that indicates nonlocality. However, the number of inequalities increases when the number of qubits increases. While a measurement of nonlocality depends on correlations, an Entanglement Witness is an operator corresponding to a physical observable. The first GHZ state-analyzer was proposed in [160] where two of the eight GHZ states can be distinguished by using linear optical elements. After this first step, several contributions were reported. In the [161], a scheme for a universal tripartite GHZ state analyzer using two-photon polarization QND is presented⁹ employing parity detectors based on weak nonlinearity. The method allows for discrimination of all eight states with a probability near 1.

In [163], a method to construct a nondestructive n -qubit GHZ state analyzer is presented. The proposal of a GHZ state analyzer using only linear-optics elements through hyperentangled states¹⁰ with polarization and momentum degrees of freedom can be found in [166]. Another scheme involving GHZ hyperentangled states was proposed recently [167]. In [168], the existence of tripartite entanglement in a noninteracting Fermi gas was investigated and some Entanglement Witnesses were introduced in that scenario. A recent study on separability criteria of three-qubit GHZ states can be accessed in [169]. In [170], sufficient conditions for detecting genuine tripartite entanglement are established that provide an operational point of view to measure and detect this type of entanglement. Experimental schemes to identify the entanglement classes of tripartite states can be accessed in [171,172]. A powerful tool to describe a density matrix of a system is the method known as quantum state tomography, which allows for the characterization of a quantum state [173]. These methods have been employed in the study of tripartite entangled states. In [174], an experimental tomographic reconstruction of a three-photon polarization GHZ state was realized. The more recent work [175] uses the method for GHZ states. In [176], a scheme for the experimental generation of a W state was introduced alongside its full characterization by using a quantum state tomography method.

8. Remote Preparation

Besides the quantum teleportation protocol, an additional type of protocol dealing with the quantum state transfer is the remote preparation protocol (RSP) [177]. There are several possibilities of implementing RSP involving different kinds of channels. It is possible to use RSP to prepare single-qubit states and states with two or more qubits [178]. Currently, this topic is studied by considering the preparation of multipartite entangled states. It is an interesting task since the remote production of entanglement can help to use this resource to establish quantum communication between distant multi-users and establish quantum distributed computation [179]. For instance, two non-maximally entangled three-qubit GHZ states can be used to prepare a four-qubit GHZ state [180] remotely. The remote preparation of a three-qubit state by using GHZ states was considered in [181]. GHZ states can also be used as the quantum channel for the remote preparation of arbitrary states of one and two qubits [182]. In [183], two maximally entangled GHZ states are employed as

⁹ Here, QND means Quantum Non-demolition related to the idea of a QND measurement [162].

¹⁰ Hyperentanglement is a type of entanglement dealing with multiple different degrees of freedom of a system. More details can be found in [164,165].

the quantum channel for the remote preparation of an arbitrary equatorial two-qubit state. A scheme for preparing atomic states remotely by using GHZ states is also possible [184]. In [185], W states are used for the remote preparation of single and two-qubit states. A scheme for the remote preparation of a two-qubit state by using two W-type states as the quantum channel was developed, as well [186]. The remote preparation of m -qubit states by using non-maximally GHZ entangled states was studied in [187]. In [188], an experimental demonstration of remote preparation of three-photon entangled states by using a single photon measurement was reported on. In [189], a scheme of joint remote preparation of an m -qubit state by using a d -dimensional GHZ state was presented. In [190], EPR pairs are used as the quantum channel to preparing an arbitrary three-qubit state. Tripartite entangled states can not only be employed to remotely prepare single and two-qubit states, but they can also be remotely prepared themselves. In [191], a scheme for preparing W states remotely by using two four-particle GHZ states as the quantum channel was presented. A proposal to remotely preparing a three-particle state by employing a three-particle orthonormal basis projective measurement can be accessed in [192]. An idea for remotely preparing W states of three and four qubits using tripartite GHZ states was presented in [193]. In [194], an efficient scheme for the remote preparation of a 2^n -qubit W state via n three-qubit GHZ states was provided. A scheme to prepare a tripartite equatorial state by using three maximally entangled GHZ states was proposed in [195]. In [196], a protocol for remotely preparing a tripartite W-type state by using an eight-qubit state as the quantum resource was presented.

9. Continuous-Variable Systems

To this point, we have explored several aspects involving tripartite entanglement of discrete variables, which refers to qubit-based developments such as photon polarization or the spin of the electron. It is worth noting that it is also possible to deal with multipartite entangled states in the domain of continuous variables [197,198]. Several quantum information protocols have been considered in this domain where the variables have a continuous spectrum of eigenvalues. For instance, an analysis of quantum teleportation of quantum states with continuous variables was presented in [199]. In [200], an experimental investigation of this subject was reported on. Entanglement swapping that involves continuous variables was investigated in [201] and [202]. A study that develops necessary conditions of separability of a multiparty continuous-variable state can be found in [203]. A detailed discussion on quantum information and continuous variables is presented in [204]. In [205], criteria were derived to detect genuine multipartite entanglement by using continuous-variable measurements including the continuous-variable GHZ state. A complete analysis of three-mode Gaussian entangled states is shown in [206]. In that work, the counterparts of GHZ and W states in the continuous-variable scenario are presented. Experimentally, the creation of a tripartite entangled state in continuous variables was realized [207]. In [208], the generation of entanglement among three beams of light with different wavelengths was demonstrated. Reference [209] reports on the experimental demonstration of tripartite entanglement where correlations involving energies and emission times of photons occur. In [210], hierarchies of separability criteria of multipartite entanglement for continuous-variable states are discussed. Recently, the development of a full quantum description of triple-photon states in the continuous-variable domain was presented in [211].

10. Noisy Environments

If we desire to consider more realistic scenarios of generation and detection as well as more realistic designs of protocols involving entanglement, we need to include some effects of the environment. Due to the interaction between the system of interest and the environment, several errors can affect the quality of the quantum protocols. The effect of decoherence, for example, can degrade the entanglement of quantum channels. Thus, several works have analyzed the noise effect in the execution of quantum protocols. Examples of noisy quantum teleportation protocols can be accessed in [212,213]. The effect of noise in tasks dealing with tripartite entanglement has also been attracting attention. For example, the influence of bit-flip noise in the entanglement and nonlocality of GHZ states was investigated in a

recent work [214]. In [215], the decay of entanglement of N -particle GHZ states due the interaction with the environment was considered. The impact of a decoherence process on the entanglement of GHZ and W states was analyzed in [216]. In [217], the quantum discord of a W state in the presence of noise was studied. The evolution of the quantum discord under noisy effects to GHZ and W states is analyzed in [218]. In [219], some properties of GHZ and W states under a depolarizing noise are discussed. In [220], noise effects on the quantum correlations of a three-qubit system was studied. A comparison between GHZ and W noisy channels that execute the quantum teleportation of a single-qubit state can be accessed in references [221,222]. In [223], the effect of the generalized amplitude damping channel on GHZ states was investigated. In [224], the problem of teleporting an unknown atomic state through a noisy GHZ channel was addressed. The entanglement of GHZ states with decoherence in non-inertial frames is discussed in [225]. In [226], the quantum teleportation by using noisy bipartite and tripartite entangled states was studied where one of the users experiments with a uniform acceleration.

In [227], schemes based on GHZ states are presented to make quantum secret sharing protocols immune to some kinds of collective noise. Effects of a particular type of noise in GHZ channels on remote preparation of states has also been investigated for a single-qubit state [228,229] and a two-qubit state [230,231]. In [232], GHZ states are considered for remote state preparation of quantum states in noisy environments. The relationship between weak measurements and GHZ entanglement distribution in the presence of noise was also investigated [233]. The robustness of GHZ and W states against decoherence was studied experimentally in [234]. In [235], a scheme for quantum communication in noisy environments by using a hybrid channel Bell-GHZ was presented. Teleportation of a GHZ state in the presence of noisy channels was analyzed in [236]. Finally, the robustness of cat-like states under Pauli noises was explored in [237].

11. Conclusions

In this work, we have addressed several aspects of tripartite entanglement with a special focus on discrete systems. We have started revisiting the main properties of this type of entanglement. We have also made some remarks on bipartite entanglement to clarify our discussion on tripartite entanglement. Subsequently, we have explored in more detail the two inequivalent classes of tripartite entanglement, namely GHZ and W , and defined the corresponding basis. We proceeded by reviewing the relationship between Bell's Theorem and the GHZ states. After that, we stated some examples of quantum information protocols working with tripartite entanglement. We gave special attention to quantum teleportation protocols, performing some calculations and exhibiting several possible schemes. After this, we listed the main contributions to the literature relevant to the production and detection of tripartite entanglement. Then, we explored some aspects important to remote preparation protocols and reviewed several characteristics of tripartite entanglement in the continuous-variable regime. Finally, we discussed the study of tripartite entanglement in the presence of a noisy environment in several scenarios.

Author Contributions: M.M.C. performed the calculations in Section 5, and wrote Sections 6–11. A.F. wrote Sections 2 and 3. M.M.C. and A.F. wrote Sections 1, 4 and 5. E.O.S. checked the calculations, revised the text, and designed all the figures.

Funding: This work was partially supported by the Brazilian agencies CAPES, CNPq, and FAPEMA. EOS acknowledges CNPq Grants 427214/2016-5 and 303774/2016-9, and FAPEMA Grants 01852/14 and 01202/16. MMC acknowledges CAPES Grant 88887.358036/2019-00.

Acknowledgments: We thank M.G.M Moreno for useful suggestions. We are grateful to M. Schreck for the careful reading of the manuscript and all the suggestions to improve the text. We also acknowledge the referees for all the criticism, comments and suggestions.

Conflicts of Interest: The authors declare no conflict of interest.

References

1. Nielsen, M.A.; Chuang, I.L. *Quantum Computation and Quantum Information*; Cambridge University Press: New York, NY, USA, 2000.
2. Gabriel, C.; Aiello, A.; Zhong, W.; Euser, T.G.; Joly, N.Y.; Banzer, P.; Förtsch, M.; Elser, D.; Andersen, U.L.; Marquardt, C.; et al. Entangling different degrees of freedom by quadrature squeezing cylindrically polarized modes. *Phys. Rev. Lett.* **2011**, *106*, 060502. [[CrossRef](#)]
3. Barnett, S. *Quantum Information*; Oxford University Press: New York, NY, USA, 2009.
4. Luo, Y.H.; Zhong, H.S.; Erhard, M.; Wang, X.L.; Peng, L.C.; Krenn, M.; Jiang, X.; Li, L.; Liu, N.L.; Lu, C.Y.; et al. Quantum teleportation in high dimensions. *Phys. Rev. Lett.* **2019**, *123*, 070505. [[CrossRef](#)]
5. Chen, P.X.; Zhu, S.Y.; Guo, G.C. General form of genuine multipartite entanglement quantum channels for teleportation. *Phys. Rev. A* **2006**, *74*, 032324. [[CrossRef](#)]
6. De, A.S.; Sen, U. Quantum Advantage in Communication Networks. Available online: <https://arxiv.org/abs/1105.2412> (accessed on 26 September 2019).
7. Raussendorf, R.; Briegel, H.J. A one-way quantum computer. *Phys. Rev. Lett.* **2001**, *86*, 5188–5191. [[CrossRef](#)]
8. Li, M.; Jia, L.; Wang, J.; Shen, S.; Fei, S.M. Measure and detection of genuine multipartite entanglement for tripartite systems. *Phys. Rev. A* **2017**, *96*, 052314. [[CrossRef](#)]
9. Briegel, H.J.; Browne, D.E.; Dür, W.; Raussendorf, R.; Van den Nest, M. Measurement-based quantum computation. *Nat. Phys.* **2009**, *5*, 19. [[CrossRef](#)]
10. Bengtsson, I.; Życzkowski, K. A Brief Introduction to Multipartite Entanglement. Available online: <https://arxiv.org/abs/1612.07747> (accessed on 26 September 2019).
11. Enríquez, M.; Wintrowicz, I.; Życzkowski, K. Maximally entangled multipartite states: A brief survey. *J. Phys. Conf. Ser.* **2016**, *698*, 012003. [[CrossRef](#)]
12. Amico, L.; Fazio, R.; Osterloh, A.; Vedral, V. Entanglement in many-body systems. *Rev. Mod. Phys.* **2008**, *80*, 517–576. [[CrossRef](#)]
13. Walter, M.; Gross, D.; Eisert, J. Multi-Partite Entanglement. Available online: <https://arxiv.org/abs/1612.02437> (accessed on 26 September 2019).
14. Fortes, R.; Rigolin, G. Fighting noise with noise in realistic quantum teleportation. *Phys. Rev. A* **2015**, *92*, 012338. [[CrossRef](#)]
15. Einstein, A.; Podolsky, B.; Rosen, N. Can quantum-mechanical description of physical reality be considered complete? *Phys. Rev.* **1935**, *47*, 777–780. [[CrossRef](#)]
16. Bennett, C.H.; Wiesner, S.J. Communication via one- and two-particle operators on Einstein-Podolsky-Rosen states. *Phys. Rev. Lett.* **1992**, *69*, 2881–2884. [[CrossRef](#)]
17. Bennett, C.H.; Brassard, G.; Crépeau, C.; Jozsa, R.; Peres, A.; Wootters, W.K. Teleporting an unknown quantum state via dual classical and Einstein-Podolsky-Rosen channels. *Phys. Rev. Lett.* **1993**, *70*, 1895–1899. [[CrossRef](#)]
18. Barreiro, J.T.; Wei, T.C.; Kwiat, P.G. Beating the channel capacity limit for linear photonic superdense coding. *Nat. Phys.* **2008**, *4*, 282. [[CrossRef](#)]
19. Takesue, H.; Dyer, S.D.; Stevens, M.J.; Verma, V.; Mirin, R.P.; Nam, S.W. Quantum teleportation over 100 km of fiber using highly efficient superconducting nanowire single-photon detectors. *Optica* **2015**, *2*, 832–835. [[CrossRef](#)]
20. Werner, R.F. Quantum states with Einstein-Podolsky-Rosen correlations admitting a hidden-variable model. *Phys. Rev. A* **1989**, *40*, 4277–4281. [[CrossRef](#)]
21. Horodecki, M.; Horodecki, P. Reduction criterion of separability and limits for a class of distillation protocols. *Phys. Rev. A* **1999**, *59*, 4206–4216. [[CrossRef](#)]
22. Brunner, N.; Cavalcanti, D.; Pironio, S.; Scarani, V.; Wehner, S. Bell nonlocality. *Rev. Mod. Phys.* **2014**, *86*, 419–478. [[CrossRef](#)]
23. Hirsch, F.; Quintino, M.T.; Vértesi, T.; Navascués, M.; Brunner, N. Better local hidden variable models for two-qubit Werner states and an upper bound on the Grothendieck constant $\alpha_K(3)$. *Quantum* **2016**, *1*, 3. [[CrossRef](#)]
24. Zhao, M.J.; Zhang, T.G.; Li-Jost, X.; Fei, S.M. Identification of three-qubit entanglement. *Phys. Rev. A* **2013**, *87*, 012316. [[CrossRef](#)]
25. Bose, S.; Vedral, V.; Knight, P.L. Purification via entanglement swapping and conserved entanglement. *Phys. Rev. A* **1999**, *60*, 194–197. [[CrossRef](#)]

26. Vidal, G. Entanglement of pure states for a single copy. *Phys. Rev. Lett.* **1999**, *83*, 1046–1049. [[CrossRef](#)]
27. Greenberger, D.M.; Horne, M.A.; Shimony, A.; Zeilinger, A. Bell's theorem without inequalities. *Am. J. Phys.* **1990**, *58*, 1131–1143. [[CrossRef](#)]
28. Greenberger, D.M.; Horne, M.A.; Zeilinger, A. Going beyond Bell's theorem. In *Bell's Theorem, Quantum Theory and Conceptions of the Universe*; Springer: Dordrecht, The Netherlands, 1989; pp. 69–72.
29. Dür, W.; Vidal, G.; Cirac, J.I. Three qubits can be entangled in two inequivalent ways. *Phys. Rev. A* **2000**, *62*, 062314. [[CrossRef](#)]
30. Żukowski, M.; Zeilinger, A.; Horne, M.; Weinfurter, H. Quest for GHZ states. *Acta Phys. Pol. A* **1998**, *93*, 187. [[CrossRef](#)]
31. Horodecki, R.; Horodecki, P.; Horodecki, M.; Horodecki, K. Quantum entanglement. *Rev. Mod. Phys.* **2009**, *81*, 865–942. [[CrossRef](#)]
32. Schwemmer, C.; Knips, L.; Tran, M.C.; De Rosier, A.; Laskowski, W.; Paterek, T.; Weinfurter, H. Genuine multipartite entanglement without multipartite correlations. *Phys. Rev. Lett.* **2015**, *114*, 180501. [[CrossRef](#)]
33. Sheng, Y.B.; Zhou, L.; Zhao, S.M. Efficient two-step entanglement concentration for arbitrary W states. *Phys. Rev. A* **2012**, *85*, 042302. [[CrossRef](#)]
34. Sheng, Y.B.; Zhou, L. Efficient W-state entanglement concentration using quantum-dot and optical microcavities. *J. Opt. Soc. Am. B* **2013**, *30*, 678–686. [[CrossRef](#)]
35. Sheng, Y.; Pan, J.; Guo, R.; Zhou, L.; Wang, L. Efficient N-particle W state concentration with different parity check gates. *Sci. Chin. Phys. Mech. Astron.* **2015**, *58*, 1–11. [[CrossRef](#)]
36. Sheng, Y.; Liu, J.; Zhao, S.; Zhou, L. Multipartite entanglement concentration for nitrogen-vacancy center and microtoroidal resonator system. *Chin. Sci. Bull.* **2013**, *58*, 3507–3513. [[CrossRef](#)]
37. Zhou, L. Efficient entanglement concentration for electron-spin W state with the charge detection. *Quantum Inf. Process.* **2013**, *12*, 2087–2101. [[CrossRef](#)]
38. Acín, A.; Andrianov, A.; Costa, L.; Jané, E.; Latorre, J.I.; Tarrach, R. Generalized schmidt decomposition and classification of three-quantum-bit states. *Phys. Rev. Lett.* **2000**, *85*, 1560–1563. [[CrossRef](#)]
39. Acín, A.; Andrianov, A.; Jané, E.; Tarrach, R. Three-qubit pure-state canonical forms. *J. Phys. A Math. Gen.* **2001**, *34*, 6725–6739. [[CrossRef](#)]
40. Acin, A.; Bruß, D.; Lewenstein, M.; Sanpera, A. Classification of mixed three-qubit states. *Phys. Rev. Lett.* **2001**, *87*, 040401. [[CrossRef](#)]
41. Erhard, M.; Malik, M.; Krenn, M.; Zeilinger, A. Experimental Greenberger–Horne–Zeilinger entanglement beyond qubits. *Nat. Photonics* **2018**, *12*, 759. [[CrossRef](#)]
42. Siewert, J.; Eltschka, C. Quantifying tripartite entanglement of three-qubit generalized Werner States. *Phys. Rev. Lett.* **2012**, *108*, 230502. [[CrossRef](#)]
43. Aravind, P. Borromean entanglement of the GHZ state. In *Potentiality, Entanglement and Passion-at-a-Distance*; Springer: Dordrecht, The Netherlands, 1997; pp. 53–59.
44. Kauffman, L.H.; Lomonaco, S.J., Jr. Quantum entanglement and topological entanglement. *New J. Phys.* **2002**, *4*, 73. [[CrossRef](#)]
45. Asoudeh, M.; Karimipour, V.; Memarzadeh, L.; Rezakhani, A. On a suggestion relating topological and quantum mechanical entanglements. *Phys. Lett. A* **2004**, *327*, 380–390. [[CrossRef](#)]
46. Mironov, S. Topological entanglement and knots. *Universe* **2019**, *5*, 60. [[CrossRef](#)]
47. Perseguers, S.; Cavalcanti, D.; Lapeyre, G., Jr.; Lewenstein, M.; Acín, A. Multipartite entanglement percolation. *Phys. Rev. A* **2010**, *81*, 032327. [[CrossRef](#)]
48. McCutcheon, W.; Pappa, A.; Bell, B.; McMillan, A.; Chailloux, A.; Lawson, T.; Mafu, M.; Markham, D.; Diamanti, E.; Kerenidis, I.; et al. Experimental verification of multipartite entanglement in quantum networks. *Nat. Commun.* **2016**, *7*, 13251. [[CrossRef](#)]
49. Duff, M. The black hole/qubit correspondence. *J. Phys. Conf. Ser.* **2013**, *462*, 012012. [[CrossRef](#)]
50. Borsten, L.; Duff, M.J.; Lévy, P. The black-hole/qubit correspondence: an up-to-date review. *Class. Quantum Gravity* **2012**, *29*, 224008. [[CrossRef](#)]
51. Bell, J.S. On the Einstein Podolsky Rosen paradox. *Phys. Phys. Fizika* **1964**, *1*, 195–200. [[CrossRef](#)]
52. Hensen, B.; Bernien, H.; Dréau, A.E.; Reiserer, A.; Kalb, N.; Blok, M.S.; Ruitenberg, J.; Vermeulen, R.F.; Schouten, R.N.; Abellán, C.; et al. Loophole-free Bell inequality violation using electron spins separated by 1.3 kilometres. *Nature* **2015**, *526*, 682. [[CrossRef](#)]
53. Mermin, N.D. Quantum mysteries revisited. *Am. J. Phys.* **1990**, *58*, 731–734. [[CrossRef](#)]

54. Lo, H.K.; Spiller, T.; Popescu, S. *Introduction to Quantum Computation and Information*; World Scientific: Singapore, 1998.
55. Cabello, A. Bell's theorem with and without inequalities for the three-qubit Greenberger-Horne-Zeilinger and W states. *Phys. Rev. A* **2002**, *65*, 032108. [[CrossRef](#)]
56. Hardy, L. Nonlocality for 2 Particles without Inequalities for Almost-All Entangled States. *Phys. Rev. Lett.* **1993**, *71*, 1665–1668. [[CrossRef](#)]
57. Mermin, N.D. Extreme quantum entanglement in a superposition of macroscopically distinct states. *Phys. Rev. Lett.* **1990**, *65*, 1838–1840. [[CrossRef](#)]
58. Ardehali, M. Bell inequalities with a magnitude of violation that grows exponentially with the number of particles. *Phys. Rev. A* **1992**, *46*, 5375–5378. [[CrossRef](#)]
59. Belinskii, A.V.; Klyshko, D.N. Interference of light and Bell's theorem. *Phys. Usp.* **1993**, *36*, 653–693. [[CrossRef](#)]
60. Svetlichny, G. Distinguishing three-body from two-body nonseparability by a Bell-type inequality. *Phys. Rev. D* **1987**, *35*, 3066–3069. [[CrossRef](#)]
61. Cereceda, J.L. Three-particle entanglement versus three-particle nonlocality. *Phys. Rev. A* **2002**, *66*, 024102. [[CrossRef](#)]
62. Bancal, J.D.; Barrett, J.; Gisin, N.; Pironio, S. Definitions of multipartite nonlocality. *Phys. Rev. A* **2013**, *88*, 014102. [[CrossRef](#)]
63. Paul, B.; Mukherjee, K.; Sarkar, D. Revealing hidden genuine tripartite nonlocality. *Phys. Rev. A* **2016**, *94*, 052101. [[CrossRef](#)]
64. Pan, J.W.; Bouwmeester, D.; Daniell, M.; Weinfurter, H.; Zeilinger, A. Experimental test of quantum nonlocality in three-photon Greenberger-Horne-Zeilinger entanglement. *Nature* **2000**, *403*, 515–519. [[CrossRef](#)]
65. Lavoie, J.; Kaltenbaek, R.; Resch, K.J. Experimental violation of Svetlichny's inequality. *New J. Phys.* **2009**, *11*, 073051. [[CrossRef](#)]
66. Erven, C.; Meyer-Scott, E.; Fisher, K.; Lavoie, J.; Higgins, B.; Yan, Z.; Pugh, C.; Bourgoin, J.P.; Prevedel, R.; Shalm, L.; et al. Experimental three-photon quantum nonlocality under strict locality conditions. *Nat. Photonics* **2014**, *8*, 292. [[CrossRef](#)]
67. Zhang, C.; Zhang, C.J.; Huang, Y.F.; Hou, Z.B.; Liu, B.H.; Li, C.F.; Guo, G.C. Experimental test of genuine multipartite nonlocality under the no-signalling principle. *Sci. Rep.* **2016**, *6*, 39327. [[CrossRef](#)]
68. Singh, P.; Kumar, A. Analysing nonlocality robustness in multiqubit systems under noisy conditions and weak measurements. *Quantum Inf. Process.* **2018**, *17*, 249. [[CrossRef](#)]
69. Swain, M.; Rai, A.; Behera, B.K.; Panigrahi, P.K. Experimental demonstration of the violations of Mermin's and Svetlichny's inequalities for W and GHZ states. *Quantum Inf. Process.* **2019**, *18*, 218. [[CrossRef](#)]
70. Caban, P.; Trzcińska, K. Noise resistance of activation of the violation of the Svetlichny inequality. *Quantum Inf. Process.* **2019**, *18*, 139. [[CrossRef](#)]
71. Chaves, R.; Cavalcanti, D.; Aolita, L. Causal hierarchy of multipartite Bell nonlocality. *Quantum* **2017**, *1*, 23. [[CrossRef](#)]
72. Karlsson, A.; Bourennane, M. Quantum teleportation using three-particle entanglement. *Phys. Rev. A* **1998**, *58*, 4394. [[CrossRef](#)]
73. Almeida, N.; Maia, L.; Villas-Bôas, C.; Moussa, M. One-cavity scheme for atomic-state teleportation through GHZ states. *Phys. Lett. A* **1998**, *241*, 213–217. [[CrossRef](#)]
74. Choudhury, B.S.; Samanta, S. Simultaneous perfect teleportation of three 2-qubit states. *Quantum Inf. Process.* **2017**, *16*, 230. [[CrossRef](#)]
75. Moreno, M.; Fonseca, A.; Cunha, M.M. Using three-partite GHZ states for partial quantum error detection in entanglement-based protocols. *Quantum Inf. Process.* **2018**, *17*, 191. [[CrossRef](#)]
76. Man, Z.X.; Xia, Y.J.; An, N.B. Quantum state sharing of an arbitrary multiqubit state using nonmaximally entangled GHZ states. *Eur. Phys. J. D* **2007**, *42*, 333–340. [[CrossRef](#)]
77. Wang, Z.Y.; Gou, Y.T.; Hou, J.X.; Cao, L.K.; Wang, X.H. Probabilistic resumable quantum teleportation of a two-qubit entangled state. *Entropy* **2019**, *21*, 352. [[CrossRef](#)]
78. Gorbachev, V.; Trubilko, A. Quantum teleportation of an Einstein-Podolsky-Rosen pair using an entangled three-particle state. *J. Exp. Theor. Phys.* **2000**, *91*, 894–898. [[CrossRef](#)]
79. Shi, B.S.; Jiang, Y.K.; Guo, G.C. Probabilistic teleportation of two-particle entangled state. *Phys. Lett. A* **2000**, *268*, 161–164. [[CrossRef](#)]

80. Tsai, C.W.; Hwang, T. Teleportation of a pure EPR state via GHZ-like state. *Int. J. Theor. Phys.* **2010**, *49*, 1969–1975. [[CrossRef](#)]
81. Li, D.f.; Wang, R.j.; Baagyere, E. Quantum teleportation of an arbitrary two-qubit state by using two three-qubit GHZ states and the six-qubit entangled state. *Quantum Inf. Process.* **2019**, *18*, 147. [[CrossRef](#)]
82. Dai, H.Y.; Chen, P.X.; Li, C.Z. Probabilistic teleportation of an arbitrary two-particle state by a partially entangled three-particle GHZ state and W state. *Opt. Commun.* **2004**, *231*, 281–287. [[CrossRef](#)]
83. Wang, K.; Yu, X.T.; Zhang, Z.C. Teleportation of two-qubit entangled state via non-maximally entangled GHZ state. *Procedia Comput. Sci.* **2018**, *131*, 1202–1208. [[CrossRef](#)]
84. Hassanpour, S.; Houshmand, M. Bidirectional teleportation of a pure EPR state by using GHZ states. *Quantum Inf. Process.* **2016**, *15*, 905–912. [[CrossRef](#)]
85. Zou, Z.Z.; Yu, X.T.; Gong, Y.X.; Zhang, Z.C. Multihop teleportation of two-qubit state via the composite GHZ–Bell channel. *Phys. Lett. A* **2017**, *381*, 76–81. [[CrossRef](#)]
86. Wang, K.; Yu, X.T.; Cai, X.F.; Zhang, Z.C. Probabilistic teleportation of arbitrary two-qubit quantum state via non-symmetric quantum channel. *Entropy* **2018**, *20*, 238. [[CrossRef](#)]
87. Xia, Y.; Song, J.; Lu, P.M.; Song, H.S. Teleportation of an N-photon Greenberger-Horne-Zeilinger (GHZ) polarization-entangled state using linear optical elements. *J. Opt. Soc. Am. B* **2010**, *27*, A1–A6. [[CrossRef](#)]
88. Hong, L. Probabilistic teleportation of the three-particle entangled state via entanglement swapping. *Chin. Phys. Lett.* **2001**, *18*, 1004. [[CrossRef](#)]
89. Xiu, L.; Hong-Cai, L. Probabilistic teleportation of a three-particle GHZ state via two three-particle entangled W states. *Commun. Theor. Phys.* **2006**, *45*, 1018. [[CrossRef](#)]
90. Choudhury, B.S.; Samanta, S. A Teleportation Protocol For Transfer of Arbitrary GHZ-states Using Intermediate Nodes. *Int. J. Theor. Phys.* **2018**, *57*, 2665–2675. [[CrossRef](#)]
91. Jin-Ming, L.; Guang-Can, G. Quantum teleportation of a three-particle entangled state. *Chin. Phys. Lett.* **2002**, *19*, 456. [[CrossRef](#)]
92. Fang, J.; Lin, Y.; Zhu, S.; Chen, X. Probabilistic teleportation of a three-particle state via three pairs of entangled particles. *Phys. Rev. A* **2003**, *67*, 014305. [[CrossRef](#)]
93. Shi, B.S.; Tomita, A. Teleportation of an unknown state by W state. *Phys. Lett. A* **2002**, *296*, 161–164. [[CrossRef](#)]
94. Joo, J.; Park, Y.J. Comment on “Teleportation of an unknown state by W states”: [Phys. Lett. A 296 (2002) 161]. *Phys. Lett. A* **2002**, *300*, 324–326. [[CrossRef](#)]
95. Shi, B.S.; Tomita, A. Reply to “Comment on: Teleportation of an unknown state by W state”. [Phys. Lett. A 300 (2002) 324]. *Phys. Lett. A* **2002**, *300*, 538–539. [[CrossRef](#)]
96. Gorbachev, V.; Trubilko, A.; Rodichkina, A.; Zhiliba, A. Can the states of the W-class be suitable for teleportation? *Phys. Lett. A* **2003**, *314*, 267–271. [[CrossRef](#)]
97. Joo, J.; Park, Y.J.; Oh, S.; Kim, J. Quantum teleportation via a W state. *New J. Phys.* **2003**, *5*, 136. [[CrossRef](#)]
98. Agrawal, P.; Pati, A. Perfect teleportation and superdense coding with W states. *Phys. Rev. A* **2006**, *74*, 062320. [[CrossRef](#)]
99. Li, L.; Qiu, D. The states of W-class as shared resources for perfect teleportation and superdense coding. *J. Phys. A Math. Theor.* **2007**, *40*, 10871. [[CrossRef](#)]
100. Zhang, Z.H.; Shu, L.; Mo, Z.W. Quantum teleportation and superdense coding through the composite W-Bell channel. *Quantum Inf. Process.* **2013**, *12*, 1957–1967. [[CrossRef](#)]
101. Zheng, Y.Z.; Gu, Y.J.; Guo, G.C. Teleportation of a three-particle entangled W state. *Chin. Phys.* **2002**, *11*, 537. [[CrossRef](#)]
102. Gao, X.; Zhang, Z.; Gong, Y.; Sheng, B.; Yu, X. Teleportation of entanglement using a three-particle entangled W state. *J. Opt. Soc. Am. B* **2017**, *34*, 142–147. [[CrossRef](#)]
103. Guo, Y.; Liu, B.H.; Li, C.F.; Guo, G.C. Advances in Quantum Dense Coding. *Adv. Quantum Technol.* **2019**, *2*, 1900011. [[CrossRef](#)]
104. Hao, J.C.; Li, C.F.; Guo, G.C. Controlled dense coding using the Greenberger-Horne-Zeilinger state. *Phys. Rev. A* **2001**, *63*, 054301. [[CrossRef](#)]
105. Huang, Y.B.; Li, S.S.; Nie, Y.Y. Controlled dense coding via GHZ-class state. *Int. J. Mod. Phys. C* **2008**, *19*, 1509–1514. [[CrossRef](#)]
106. Yang, X.; Bai, M.Q.; Mo, Z.W. Controlled Dense Coding with the W State. *Int. J. Theor. Phys.* **2017**, *56*, 3525–3533. [[CrossRef](#)]

107. Zhou, Y.S.; Wang, F.; Luo, M.X. Efficient Superdense Coding with W States. *Int. J. Theor. Phys.* **2018**, *57*, 1935–1941. [[CrossRef](#)]
108. Ye, L.; Yu, L.B. Scheme for implementing quantum dense coding using tripartite entanglement in cavity QED. *Phys. Lett. A* **2005**, *346*, 330–336. [[CrossRef](#)]
109. Roy, S.; Chanda, T.; Das, T.; De, A.S.; Sen, U. Deterministic quantum dense coding networks. *Phys. Lett. A* **2018**, *382*, 1709–1715. [[CrossRef](#)]
110. Wiesner, S. Conjugate coding. *ACM Spec. Interest Group Algorithms Comput. Theor. News* **1983**, *15*, 78–88. [[CrossRef](#)]
111. Bennett, C.H.; Brassard, G. Quantum cryptography: public key distribution and coin tossing. *Theor. Comput. Sci.* **2014**, *560*, 7–11. [[CrossRef](#)]
112. Ekert, A.K. Quantum cryptography based on Bell's theorem. *Phys. Rev. Lett.* **1991**, *67*, 661. [[CrossRef](#)] [[PubMed](#)]
113. Hillery, M.; Bužek, V.; Berthiaume, A. Quantum secret sharing. *Phys. Rev. A* **1999**, *59*, 1829. [[CrossRef](#)]
114. Joo, J.; Lee, J.; Jang, J.; Park, Y.J. Quantum Secure Communication with W States. Available online: <https://arxiv.org/abs/quant-ph/0204003> (accessed on 26 September 2019).
115. Jin, X.R.; Ji, X.; Zhang, Y.Q.; Zhang, S.; Hong, S.K.; Yeon, K.H.; Um, C.I. Three-party quantum secure direct communication based on GHZ states. *Phys. Lett. A* **2006**, *354*, 67–70. [[CrossRef](#)]
116. Man, Z.X.; Xia, Y.J.; An, N.B. Quantum secure direct communication by using GHZ states and entanglement swapping. *J. Phys. B At. Mol. Opt. Phys.* **2006**, *39*, 3855. [[CrossRef](#)]
117. Chen, X.B.; Wen, Q.Y.; Guo, F.Z.; Sun, Y.; Xu, G.; Zhu, F.C. Controlled quantum secure direct communication with W state. *Int. J. Quantum Inf.* **2008**, *6*, 899–906. [[CrossRef](#)]
118. Lo, H.K.; Curty, M.; Qi, B. Measurement-Device-Independent Quantum Key Distribution. *Phys. Rev. Lett.* **2012**, *108*, 130503. [[CrossRef](#)] [[PubMed](#)]
119. Fu, Y.; Yin, H.L.; Chen, T.Y.; Chen, Z.B. Long-Distance Measurement-Device-Independent Multiparty Quantum Communication. *Phys. Rev. Lett.* **2015**, *114*, 090501. [[CrossRef](#)]
120. Christandl, M.; Wehner, S. Quantum anonymous transmissions. In *International Conference on the Theory and Application of Cryptology and Information Security*; Springer: Berlin/Heidelberg, Germany, 2005; pp. 217–235.
121. Lipinska, V.; Murta, G.; Wehner, S. Anonymous transmission in a noisy quantum network using the W state. *Phys. Rev. A* **2018**, *98*, 052320. [[CrossRef](#)]
122. Cruz, D.; Fournier, R.; Gremion, F.; Jeannerot, A.; Komagata, K.; Tomic, T.; Thiesbrummel, J.; Chan, C.L.; Macris, N.; Dupertuis, M.A.; et al. Efficient quantum algorithms for GHZ and W states, and implementation on the IBM quantum computer. *Adv. Quantum Technol.* **2019**, *2*, 1900015. [[CrossRef](#)]
123. Hwang, M.R.; Park, D.; Jung, E. Tripartite entanglement in a noninertial frame. *Phys. Rev. A* **2011**, *83*, 012111. [[CrossRef](#)]
124. Acin, A.; Jane, E.; Dür, W.; Vidal, G. Optimal distillation of a Greenberger-Horne-Zeilinger state. *Phys. Rev. Lett.* **2000**, *85*, 4811. [[CrossRef](#)] [[PubMed](#)]
125. Mo, Y.N.; Li, C.F.; Guo, G.C. Distillation of the Greenberger-Horne-Zeilinger state from arbitrary tripartite states. *Phys. Rev. A* **2002**, *65*, 024301. [[CrossRef](#)]
126. Yildiz, A. Optimal distillation of three-qubit W states. *Phys. Rev. A* **2010**, *82*, 012317. [[CrossRef](#)]
127. Liao, X.P.; Fang, M.F.; Fang, J.S. Entanglement purification and amplification of three-qubit states using two-outcome weak measurements. *J. Mod. Opt.* **2014**, *61*, 1018–1026. [[CrossRef](#)]
128. Yuan, J.; Tang, S.; Wang, X.; Zhang, D. One-step distillation of local-unitary-equivalent GHZ-type states. *Quantum Inf. Process.* **2018**, *17*, 259. [[CrossRef](#)]
129. Gottesman, D.; Chuang, I.L. Demonstrating the viability of universal quantum computation using teleportation and single-qubit operations. *Nature* **1999**, *402*, 390. [[CrossRef](#)]
130. Cai, Y.; Le, H.N.; Scarani, V. State complexity and quantum computation. *Annalen der Physik* **2015**, *527*, 684–700. [[CrossRef](#)]
131. D'Hondt, E.; Panangaden, P. The Computational Power of the W And GHZ States. *Quantum Inf. Comput.* **2006**, *6*, 173–183.
132. Rajan, D.; Visser, M. Quantum Blockchain using entanglement in time. *Quantum Rep.* **2019**, *1*, 2. [[CrossRef](#)]
133. Zhao, Z.; Chen, Y.A.; Zhang, A.N.; Yang, T.; Briegel, H.J.; Pan, J.W. Experimental demonstration of five-photon entanglement and open-destination teleportation. *Nature* **2004**, *430*, 54–58. [[CrossRef](#)] [[PubMed](#)]

134. Monz, T.; Schindler, P.; Barreiro, J.T.; Chwalla, M.; Nigg, D.; Coish, W.A.; Harlander, M.; Hänsel, W.; Hennrich, M.; Blatt, R. 14-qubit entanglement: Creation and coherence. *Phys. Rev. Lett.* **2011**, *106*, 130506. [[CrossRef](#)]
135. Bouwmeester, D.; Pan, J.W.; Daniell, M.; Weinfurter, H.; Zeilinger, A. Observation of three-photon Greenberger-Horne-Zeilinger entanglement. *Phys. Rev. Lett.* **1999**, *82*, 1345. [[CrossRef](#)]
136. Eibl, M.; Kiesel, N.; Bourennane, M.; Kurtsiefer, C.; Weinfurter, H. Experimental Realization of a Three-Qubit Entangled W State. *Phys. Rev. Lett.* **2004**, *92*, 077901. [[CrossRef](#)] [[PubMed](#)]
137. Zeilinger, A.; Horne, M.A.; Weinfurter, H.; Żukowski, M. Three-particle entanglements from two entangled pairs. *Phys. Rev. Lett.* **1997**, *78*, 3031. [[CrossRef](#)]
138. Laflamme, R.; Knill, E.; Zurek, W.; Catasti, P.; Mariappan, S. NMR Greenberger-Horne-Zeilinger states. *Philos. Trans. R. Soc. Lond. Ser. A* **1998**, *356*, 1941–1948. [[CrossRef](#)]
139. Ju, L.; Yang, M.; Paunković, N.; Chu, W.J.; Cao, Z.L. Creating photonic GHZ and W states via quantum walk. *Quantum Inf. Process.* **2019**, *18*, 176. [[CrossRef](#)]
140. Erdösi, D.; Huber, M.; Hiesmayr, B.C.; Hasegawa, Y. Proving the generation of genuine multipartite entanglement in a single-neutron interferometer experiment. *New J. Phys.* **2013**, *15*, 023033. [[CrossRef](#)]
141. Yamamoto, T.; Tamaki, K.; Koashi, M.; Imoto, N. Polarization-entangled W state using parametric down-conversion. *Phys. Rev. A* **2002**, *66*, 064301. [[CrossRef](#)]
142. Yu, C.S.; Yi, X.X.; Song, H.S.; Mei, D. Robust preparation of Greenberger-Horne-Zeilinger and W states of three distant atoms. *Phys. Rev. A* **2007**, *75*, 044301. [[CrossRef](#)]
143. Deng, Z.J.; Feng, M.; Gao, K.L. Simple scheme for generating an n -qubit W state in cavity QED. *Phys. Rev. A* **2006**, *73*, 014302. [[CrossRef](#)]
144. Gorbachev, V.; Rodichkina, A.; Trubilko, A.; Zhiliba, A. On preparation of the entangled W -states from atomic ensembles. *Phys. Lett. A* **2003**, *310*, 339–343. [[CrossRef](#)]
145. Roos, C.F.; Riebe, M.; Häffner, H.; Hänsel, W.; Benhelm, J.; Lancaster, G.P.; Becher, C.; Schmidt-Kaler, F.; Blatt, R. Control and measurement of three-qubit entangled states. *Science* **2004**, *304*, 1478–1480. [[CrossRef](#)]
146. Kang, Y.H.; Xia, Y.; Lu, P.M. Effective scheme for preparation of a spin-qubit Greenberger-Horne-Zeilinger state and W state in a quantum-dot-microcavity system. *J. Opt. Soc. Am. B* **2015**, *32*, 1323–1329. [[CrossRef](#)]
147. Kang, Y.H.; Chen, Y.H.; Wu, Q.C.; Huang, B.H.; Song, J.; Xia, Y. Fast generation of W states of superconducting qubits with multiple Schrödinger dynamics. *Sci. Rep.* **2016**, *6*, 36737. [[CrossRef](#)] [[PubMed](#)]
148. Chen, R.X.; Shen, L.T. Tripartite entanglement of atoms trapped in coupled cavities via quantum Zeno dynamics. *Phys. Lett. A* **2011**, *375*, 3840–3844. [[CrossRef](#)]
149. Miry, S.R.; Tavassoly, M.K.; Roknizadeh, R. Generation of some entangled states of the cavity field. *Quantum Inf. Process.* **2015**, *14*, 593–606. [[CrossRef](#)]
150. Hamel, D.R.; Shalm, L.K.; Hübel, H.; Miller, A.J.; Marsili, F.; Verma, V.B.; Mirin, R.P.; Nam, S.W.; Resch, K.J.; Jennewein, T. Direct generation of three-photon polarization entanglement. *Nat. Photonics* **2014**, *8*, 801. [[CrossRef](#)]
151. de Lima Bernardo, B.; Lencses, M.; Brito, S.; Canabarro, A. Greenberger-Horne-Zeilinger state generation with linear optical elements. *Quantum Inf. Process.* **2019**, *18*, 331. [[CrossRef](#)]
152. Heo, J.; Hong, C.; Choi, S.G.; Hong, J.P. Scheme for generation of three-photon entangled W state assisted by cross-Kerr nonlinearity and quantum dot. *Sci. Rep.* **2019**, *9*, 10151. [[CrossRef](#)] [[PubMed](#)]
153. Bellomo, B.; Lo Franco, R.; Compagno, G. N identical particles and one particle to entangle them all. *Phys. Rev. A* **2017**, *96*, 022319. [[CrossRef](#)]
154. Yesilyurt, C.; Bugu, S.; Ozaydin, F.; Altintas, A.A.; Tame, M.; Yang, L.; Özdemir, S.K. Deterministic local doubling of W states. *J. Opt. Soc. Am. B* **2016**, *33*, 2313–2319. [[CrossRef](#)]
155. Li, D.X.; Zheng, T.Y.; Shao, X.Q. Adiabatic preparation of Multipartite GHZ states via Rydberg ground-state blockade. *Opt. Express* **2019**, *27*, 20874–20885. [[CrossRef](#)] [[PubMed](#)]
156. Omran, A.; Levine, H.; Keesling, A.; Semeghini, G.; Wang, T.T.; Ebadi, S.; Bernien, H.; Zibrov, A.S.; Pichler, H.; Choi, S.; et al. Generation and Manipulation of Schrödinger Cat States in Rydberg Atom Arrays. Available online: <https://arxiv.org/abs/1905.05721> (accessed on 26 September 2019).
157. Gühne, O.; Tóth, G. Entanglement detection. *Phys. Rep.* **2009**, *474*, 1–75. [[CrossRef](#)]
158. Bruß, D.; Cirac, J.I.; Horodecki, P.; Hulpke, F.; Kraus, B.; Lewenstein, M.; Sanpera, A. Reflections upon separability and distillability. *J. Mod. Opt.* **2002**, *49*, 1399–1418. [[CrossRef](#)]
159. Gerke, S.; Vogel, W.; Sperling, J. Numerical Construction of Multipartite Entanglement Witnesses. *Phys. Rev. X* **2018**, *8*, 031047. [[CrossRef](#)]

160. Pan, J.W.; Zeilinger, A. Greenberger-Horne-Zeilinger-state analyzer. *Phys. Rev. A* **1998**, *57*, 2208. [[CrossRef](#)]
161. Qian, J.; Feng, X.L.; Gong, S.Q. Universal Greenberger-Horne-Zeilinger-state analyzer based on two-photon polarization parity detection. *Phys. Rev. A* **2005**, *72*, 052308. [[CrossRef](#)]
162. Ralph, T.C.; Bartlett, S.D.; O'Brien, J.L.; Pryde, G.J.; Wiseman, H.M. Quantum nondemolition measurements for quantum information. *Phys. Rev. A* **2006**, *73*, 012113. [[CrossRef](#)]
163. Wang, X.W.; Zhang, D.Y.; Tang, S.Q.; Xie, L.J. Nondestructive Greenberger-Horne-Zeilinger-state analyzer. *Quantum Inf. Process.* **2013**, *12*, 1065–1075. [[CrossRef](#)]
164. Barbieri, M.; Cinelli, C.; Mataloni, P.; De Martini, F. Polarization-momentum hyperentangled states: Realization and characterization. *Phys. Rev. A* **2005**, *72*, 052110. [[CrossRef](#)]
165. Bhatti, D.; von Zanthier, J.; Agarwal, G.S. Entanglement of polarization and orbital angular momentum. *Phys. Rev. A* **2015**, *91*, 062303. [[CrossRef](#)]
166. Song, S.; Cao, Y.; Sheng, Y.B.; Long, G.L. Complete Greenberger-Horne-Zeilinger state analyzer using hyperentanglement. *Quantum Inf. Process.* **2013**, *12*, 381–393. [[CrossRef](#)]
167. Zheng, Y.Y.; Liang, L.X.; Zhang, M. Self-assisted complete analysis of three-photon hyperentangled Greenberger-Horne-Zeilinger states with nitrogen-vacancy centers in microcavities. *Quantum Inf. Process.* **2018**, *17*, 172. [[CrossRef](#)]
168. Habibian, H.; Clark, J.W.; Behbood, N.; Hingerl, K. Greenberger-Horne-Zeilinger and W entanglement witnesses for the noninteracting Fermi gas. *Phys. Rev. A* **2010**, *81*, 032302. [[CrossRef](#)]
169. Chen, X.Y.; Jiang, L.Z.; Yu, P.; Tian, M. Necessary and sufficient fully separable criterion and entanglement of three-qubit Greenberger-Horne-Zeilinger diagonal states. *Quantum Inf. Process.* **2015**, *14*, 2463–2476. [[CrossRef](#)]
170. Li, M.; Wang, J.; Shen, S.; Chen, Z.; Fei, S.M. Detection and measure of genuine tripartite entanglement with partial transposition and realignment of density matrices. *Sci. Rep.* **2017**, *7*, 17274. [[CrossRef](#)]
171. Singh, A.; Singh, H.; Dorai, K. Experimental classification of entanglement in arbitrary three-qubit pure states on an NMR quantum information processor. *Phys. Rev. A* **2018**, *98*, 032301. [[CrossRef](#)]
172. Singh, A.; Dorai, K. Experimentally identifying the entanglement class of pure tripartite states. *Quantum Inf. Process.* **2018**, *17*, 334. [[CrossRef](#)]
173. Gross, D.; Liu, Y.K.; Flammia, S.T.; Becker, S.; Eisert, J. Quantum State Tomography via Compressed Sensing. *Phys. Rev. Lett.* **2010**, *105*, 150401. [[CrossRef](#)] [[PubMed](#)]
174. Resch, K.J.; Walther, P.; Zeilinger, A. Full Characterization of a Three-Photon Greenberger-Horne-Zeilinger State Using Quantum State Tomography. *Phys. Rev. Lett.* **2005**, *94*, 070402. [[CrossRef](#)] [[PubMed](#)]
175. Lu, H.X.; Zhao, J.Q.; Wang, X.Q. Characterization of a high-intensity three-qubit GHZ state using state tomography and Gisin's inequality. *Phys. Lett. A* **2011**, *375*, 1850–1854. [[CrossRef](#)]
176. Mikami, H.; Li, Y.; Fukuoka, K.; Kobayashi, T. New High-Efficiency Source of a Three-Photon W State and its Full Characterization Using Quantum State Tomography. *Phys. Rev. Lett.* **2005**, *95*, 150404. [[CrossRef](#)] [[PubMed](#)]
177. Shi, J.; Zhan, Y.B. Scheme for Asymmetric and Deterministic Controlled Bidirectional Joint Remote State Preparation. *Commun. Theor. Phys.* **2018**, *70*, 515. [[CrossRef](#)]
178. Sun, Y.R.; Chen, X.B.; Xu, G.; Yuan, K.G.; Yang, Y.X. Asymmetric controlled bidirectional remote preparation of two-and three-qubit equatorial state. *Sci. Rep.* **2019**, *9*, 2081. [[CrossRef](#)]
179. Kurpiers, P.; Magnard, P.; Walter, T.; Royer, B.; Pechal, M.; Heinsoo, J.; Salathé, Y.; Akin, A.; Storz, S.; Besse, J.C.; et al. Deterministic quantum state transfer and remote entanglement using microwave photons. *Nature* **2018**, *558*, 264. [[CrossRef](#)] [[PubMed](#)]
180. Dai, H.Y.; Chen, P.X.; Liang, L.M.; Li, C.Z. Classical communication cost and remote preparation of the four-particle GHZ class state. *Phys. Lett. A* **2006**, *355*, 285–288. [[CrossRef](#)]
181. Luo, M.X.; Chen, X.B.; Ma, S.Y.; Niu, X.X.; Yang, Y.X. Joint remote preparation of an arbitrary three-qubit state. *Opt. Commun.* **2010**, *283*, 4796–4801. [[CrossRef](#)]
182. Zhan, Y.B.; Ma, P.C. Deterministic joint remote preparation of arbitrary two-and three-qubit entangled states. *Quantum Inf. Process.* **2013**, *12*, 997–1009. [[CrossRef](#)]
183. Choudhury, B.S.; Dhara, A. Joint remote state preparation for two-qubit equatorial states. *Quantum Inf. Process.* **2015**, *14*, 373–379. [[CrossRef](#)]
184. Khosa, A.H.; Saif, F. Remote preparation of atomic and field cluster states from a pair of tri-partite GHZ states. *Chin. Phys. B* **2010**, *19*, 040309. [[CrossRef](#)]

185. An, N.B. Joint remote state preparation via W and W-type states. *Opt. Commun.* **2010**, *283*, 4113–4117. [[CrossRef](#)]
186. Wang, Z.Y. Classical communication cost and probabilistic remote two-qubit state preparation via POVM and W-type states. *Quantum Inf. Process.* **2012**, *11*, 1585–1602. [[CrossRef](#)]
187. Wang, D.; Hoehn, R.; Ye, L.; Kais, S. Generalized remote preparation of arbitrary m-qubit entangled states via genuine entanglements. *Entropy* **2015**, *17*, 1755–1774. [[CrossRef](#)]
188. Ra, Y.S.; Lim, H.T.; Kim, Y.H. Remote preparation of three-photon entangled states via single-photon measurement. *Phys. Rev. A* **2016**, *94*, 042329. [[CrossRef](#)]
189. Lv, S.X.; Zhao, Z.W.; Zhou, P. Multiparty-controlled joint remote preparation of an arbitrary m-qudit state with d-dimensional Greenberger-Horne-Zeilinger states. *Int. J. Theor. Phys.* **2018**, *57*, 148–158. [[CrossRef](#)]
190. Xia, Y.; Chen, Q.Q.; An, N.B. Deterministic joint remote preparation of an arbitrary three-qubit state via Einstein-Podolsky-Rosen pairs with a passive receiver. *J. Phys. A Math. Theor.* **2012**, *45*, 335306. [[CrossRef](#)]
191. Luo, M.X.; Chen, X.B.; Ma, S.Y.; Yang, Y.X.; Hu, Z.M. Deterministic remote preparation of an arbitrary W-class state with multiparty. *J. Phys. B At. Mol. Opt. Phys.* **2010**, *43*, 065501. [[CrossRef](#)]
192. Peng-Cheng, M.; You-Bang, Z. Scheme for probabilistic remotely preparing a multi-particle entangled GHZ state. *Chin. Phys. B* **2008**, *17*, 445. [[CrossRef](#)]
193. Wang, D.; Hu, Y.D.; Wang, Z.Q.; Ye, L. Efficient and faithful remote preparation of arbitrary three-and four-particle class entangled states. *Quantum Inf. Process.* **2015**, *14*, 2135–2151. [[CrossRef](#)]
194. Wu, N.N.; Jiang, M. A highly efficient scheme for joint remote preparation of multi-qubit W state with minimum quantum resource. *Quantum Inf. Process.* **2018**, *17*, 340. [[CrossRef](#)]
195. Sang, Z.W. Deterministic Joint Remote State Preparation of an Arbitrary Equatorial Three-Qubit State. *Int. J. Theor. Phys.* **2019**, *58*, 1157–1160. [[CrossRef](#)]
196. Choudhury, B.S.; Samanta, S. Remote Preparation of Some Three Particle Entangled States Under Divided Information. *Int. J. Theor. Phys.* **2019**, *58*, 83–91. [[CrossRef](#)]
197. Eisert, J.; Plenio, M. Introduction to the basics of entanglement theory in continuous-variable systems. *Int. J. Quantum Inf.* **2003**, *1*, 479–506. [[CrossRef](#)]
198. Adesso, G.; Illuminati, F. Entanglement in continuous-variable systems: recent advances and current perspectives. *J. Phys. A Math. Theor.* **2007**, *40*, 7821. [[CrossRef](#)]
199. Braunstein, S.L.; Kimble, H.J. Teleportation of Continuous Quantum Variables. *Phys. Rev. Lett.* **1998**, *80*, 869–872. [[CrossRef](#)]
200. Bowen, W.P.; Treps, N.; Buchler, B.C.; Schnabel, R.; Ralph, T.C.; Bachor, H.A.; Symul, T.; Lam, P.K. Experimental investigation of continuous-variable quantum teleportation. *Phys. Rev. A* **2003**, *67*, 032302. [[CrossRef](#)]
201. Polkinghorne, R.E.S.; Ralph, T.C. Continuous Variable Entanglement Swapping. *Phys. Rev. Lett.* **1999**, *83*, 2095–2099. [[CrossRef](#)]
202. Takeda, S.; Fuwa, M.; van Loock, P.; Furusawa, A. Entanglement Swapping between Discrete and Continuous Variables. *Phys. Rev. Lett.* **2015**, *114*, 100501. [[CrossRef](#)] [[PubMed](#)]
203. van Loock, P.; Furusawa, A. Detecting genuine multipartite continuous-variable entanglement. *Phys. Rev. A* **2003**, *67*, 052315. [[CrossRef](#)]
204. Adesso, G.; Ragy, S.; Lee, A.R. Continuous variable quantum information: Gaussian states and beyond. *Open Syst. Inf. Dyn.* **2014**, *21*, 1440001. [[CrossRef](#)]
205. Teh, R.Y.; Reid, M.D. Criteria for genuine N-partite continuous-variable entanglement and Einstein-Podolsky-Rosen steering. *Phys. Rev. A* **2014**, *90*, 062337. [[CrossRef](#)]
206. Adesso, G.; Serafini, A.; Illuminati, F. Multipartite entanglement in three-mode Gaussian states of continuous-variable systems: Quantification, sharing structure, and decoherence. *Phys. Rev. A* **2006**, *73*, 032345. [[CrossRef](#)]
207. Aoki, T.; Takei, N.; Yonezawa, H.; Wakui, K.; Hiraoka, T.; Furusawa, A.; van Loock, P. Experimental creation of a fully inseparable tripartite continuous-variable state. *Phys. Rev. Lett.* **2003**, *91*, 080404. [[CrossRef](#)] [[PubMed](#)]
208. Coelho, A.; Barbosa, F.; Cassemiro, K.; Villar, A.; Martinelli, M.; Nussenzveig, P. Three-color entanglement. *Science* **2009**, *326*, 823–826. [[CrossRef](#)] [[PubMed](#)]
209. Shalm, L.K.; Hamel, D.R.; Yan, Z.; Simon, C.; Resch, K.J.; Jennewein, T. Three-photon energy-time entanglement. *Nat. Phys.* **2013**, *9*, 19. [[CrossRef](#)]

210. Valido, A.A.; Levi, F.; Mintert, F. Hierarchies of multipartite entanglement for continuous-variable states. *Phys. Rev. A* **2014**, *90*, 052321. [[CrossRef](#)]
211. González, E.A.R.; Borne, A.; Boulanger, B.; Levenson, J.A.; Bencheikh, K. Continuous-Variable Triple-Photon States Quantum Entanglement. *Phys. Rev. Lett.* **2018**, *120*, 043601. [[CrossRef](#)]
212. Liang, H.Q.; Liu, J.M.; Feng, S.S.; Chen, J.G. Quantum teleportation with partially entangled states via noisy channels. *Quantum Inf. Process.* **2013**, *12*, 2671–2687. [[CrossRef](#)]
213. Fortes, R.; Rigolin, G. Probabilistic quantum teleportation in the presence of noise. *Phys. Rev. A* **2016**, *93*, 062330. [[CrossRef](#)]
214. Zhao, J.Q.; Cao, L.Z.; Yang, Y.; Li, Y.D.; Lu, H.X. Tripartite entanglement and non-locality in three-qubit Greenberger–Horne–Zeilinger states with bit-flip noise. *Can. J. Phys.* **2018**, *97*, 248–251. [[CrossRef](#)]
215. Aolita, L.; Chaves, R.; Cavalcanti, D.; Acín, A.; Davidovich, L. Scaling Laws for the Decay of Multiqubit Entanglement. *Phys. Rev. Lett.* **2008**, *100*, 080501. [[CrossRef](#)] [[PubMed](#)]
216. Kenfack, L.T.; Tchoffo, M.; Fai, L.C. Decoherence and protection of entanglement of a system of three qubits driven by a classical Gaussian distributed fluctuating field. *Phys. Lett. A* **2018**, *382*, 2805–2818. [[CrossRef](#)]
217. Guo, H.; Liu, J.M.; Zhang, C.J.; Oh, C. Quantum discord of a three-qubit w-class state in noisy environments. *Quantum Inf. Comput.* **2012**, *12*, 677.
218. Mahdian, M.; Yousefjani, R.; Salimi, S. Quantum discord evolution of three-qubit states under noisy channels. *Eur. Phys. J. D* **2012**, *66*, 133. [[CrossRef](#)]
219. Metwally, N.; Almannaei, A. Dynamics of three-qubit systems in a noisy environment. *Can. J. Phys.* **2015**, *94*, 170–176. [[CrossRef](#)]
220. Lionel, T.K.; Martin, T.; Collince, F.G.; Fai, L.C. Effects of static noise on the dynamics of quantum correlations for a system of three qubits. *Int. J. Mod. Phys. B* **2017**, *31*, 1750046. [[CrossRef](#)]
221. Jung, E.; Hwang, M.R.; Ju, Y.H.; Kim, M.S.; Yoo, S.K.; Kim, H.; Park, D.; Son, J.W.; Tamaryan, S.; Cha, S.K. Greenberger-Horne-Zeilinger versus W states: Quantum teleportation through noisy channels. *Phys. Rev. A* **2008**, *78*, 012312. [[CrossRef](#)]
222. Hu, M.L. Robustness of Greenberger–Horne–Zeilinger and W states for teleportation in external environments. *Phys. Lett. A* **2011**, *375*, 922–926. [[CrossRef](#)]
223. Metwally, N. Entanglement and quantum teleportation via decohered tripartite entangled states. *Ann. Phys.* **2014**, *351*, 704–713. [[CrossRef](#)]
224. Chun, M.; Ming, Y.; Zhuo-Liang, C. Controlled Quantum Teleportation Through Noisy GHZ Channel. *Commun. Theor. Phys.* **2010**, *53*, 489. [[CrossRef](#)]
225. Khan, S. Entanglement of tripartite states with decoherence in non-inertial frames. *J. Mod. Opt.* **2012**, *59*, 250–258. [[CrossRef](#)]
226. Zounia, M.; Shamirzaie, M.; Ashouri, A. Quantum teleportation via noisy bipartite and tripartite accelerating quantum states: beyond the single mode approximation. *J. Phys. A Math. Theor.* **2017**, *50*, 395302. [[CrossRef](#)]
227. Yang, Y.G.; Gao, S.; Li, D.; Zhou, Y.H.; Shi, W.M. Three-party quantum secret sharing against collective noise. *Quantum Inf. Process.* **2019**, *18*, 215. [[CrossRef](#)]
228. Liang, H.Q.; Liu, J.M.; Feng, S.S.; Chen, J.G. Remote state preparation via a GHZ-class state in noisy environments. *J. Phys. B At. Mol. Opt. Phys.* **2011**, *44*, 115506. [[CrossRef](#)]
229. Liang, H.Q.; Liu, J.M.; Feng, S.S.; Chen, J.G.; Xu, X.Y. Effects of noises on joint remote state preparation via a GHZ-class channel. *Quantum Inf. Process.* **2015**, *14*, 3857–3877. [[CrossRef](#)]
230. Zhong-Fang, C.; Jin-Ming, L.; Lei, M. Deterministic joint remote preparation of an arbitrary two-qubit state in the presence of noise. *Chin. Phys. B* **2013**, *23*, 020312.
231. Qu, Z.; Wu, S.; Wang, M.; Sun, L.; Wang, X. Effect of quantum noise on deterministic remote state preparation of an arbitrary two-particle state via various quantum entangled channels. *Quantum Inf. Process.* **2017**, *16*, 306. [[CrossRef](#)]
232. Zhang, C.Y.; Bai, M.Q.; Zhou, S.Q. Cyclic joint remote state preparation in noisy environment. *Quantum Inf. Process.* **2018**, *17*, 146. [[CrossRef](#)]
233. Wang, X.W.; Yu, S.; Zhang, D.Y.; Oh, C. Effect of weak measurement on entanglement distribution over noisy channels. *Sci. Rep.* **2016**, *6*, 22408. [[CrossRef](#)] [[PubMed](#)]
234. Singh, H.; Dorai, K. Evolution of tripartite entangled states in a decohering environment and their experimental protection using dynamical decoupling. *Phys. Rev. A* **2018**, *97*, 022302. [[CrossRef](#)]

235. Jiang, S.X.; Zhou, R.G.; Xu, R.; Luo, G. Cyclic Hybrid Double-Channel Quantum Communication via Bell-State and GHZ-State in Noisy Environments. *IEEE Access* **2019**, *7*, 80530–80541. [[CrossRef](#)]
236. Cunha, M.M.; Fonseca, E.; Moreno, M.; Parisio, F. Non-ideal teleportation of tripartite entanglement: Einstein–Podolsky–Rosen versus Greenberger–Horne–Zeilinger schemes. *Quantum Inf. Process.* **2017**, *16*, 254. [[CrossRef](#)]
237. Wang, X.W.; Tang, S.Q.; Liu, Y.; Yuan, J.B. Improving the Robustness of Entangled States by Basis Transformation. *Entropy* **2019**, *21*, 59. [[CrossRef](#)]



© 2019 by the authors. Licensee MDPI, Basel, Switzerland. This article is an open access article distributed under the terms and conditions of the Creative Commons Attribution (CC BY) license (<http://creativecommons.org/licenses/by/4.0/>).